EUROPEAN CENTRE FOR MEDIUM RANGE WEATHER FORECASTS

TECHNICAL REPORT
****
NO. 4
*****

MARCH

1977

****

***

*

A Model for Medium Range Weather Forecasting

- Adiabatic Formulation -

By

D.M. Burridge and J. Haseler

European Centre for Medium Range Weather Forecasts

Fitzwilliam House
Skimped Hill
Bracknell, Berks.
United Kingdom

CONTENTS PAGE NUMBER

ABSTRACT

In this report the design of the finite difference scheme for ECMWF's first global model using the primitive equations in spherical co-ordinates is described. The spatial differencing scheme is formulated in accordance with methods which are now well established and maintains many of the more important integral constraints satisfied by the continuous forms of the equation. The maintenance of these constraints inhibits non-linear instability and ensures a more accurate simulation of exchange and cascade processes.

The results of an adiabatic integration to three days and an integration to ten days with a simple surface drag formulation and convective adjustment scheme are presented.

Although not discussed in this paper, a high resolution limited area version of the model has been designed. This model will be used primarily for experiments with the model's parameterisation schemes for sub-grid scale phenomena.

1. Introduction

Meteorologists are faced with a wide, though unenviable, choice of schemes for the basic building blocks of a numerical weather prediction model, whether it is to be used for research or operational forecasting. For the spatial representation the main areas of choice are grid point schemes, pseudo-spectral or functional approaches or Galerkin techniques using either local (for example finite elements) or global (for example true spectral) basis functions. For medium range weather forecasting not only is the accuracy of the initial data important in order to provide an accurate description of the evolution of the atmosphere in the early stages of the forecast, but a proper representation, achieved mainly through sub-grid scale parameterisations, of all the important physical processes for the atmosphere is necessary to determine the development areas of new systems not present in the initial data. In the area of physical parameterisation the variety and levels of sophistication are enormous. In this paper we confine ourselves to a description of a formulation for an adiabatic calculation. The formulation for the diabatic part will follow in another technical report.

For the first operational model and for most of our research for the next few years we have chosen a grid point representation with second order difference approximations for the spatial derivatives. The model can be used in global or hemispheric (with a solid wall boundary condition at the equator) domains. In addition a limited area version is available which uses a relaxation technique described by DAVIES (1976). In the limited area version the model's dependent variables are relaxed towards externally specified values within a narrow boundary zone. This technique provides possibly a better alternative to the solid wall equatorial boundary condition for hemispheric integrations. In this case the model could be relaxed within a narrow equatorial band towards a combination of persistence and climatology or even towards values obtained from a global forecast produced by a coarse mesh integration. A preliminary description of the limited area version is available in an internal report by KÅLLBERG (1977).

The spatial differencing scheme has been designed to preserve many of the important integral constraints satisfied by the continuous equations; conservation of mass, conservation of moisture, conservation of potential absolute enstrophy during potential vorticity advection by the horizontal wind field and conservation of total energy apart from sources, sinks and boundary fluxes. Maintenance of integral constraints is probably not strictly necessary for short range forecasting in which the concern is with the accuracy of the local description. However, for longer term integrations maintenance of these constraints is essential in order to prevent systematic errors and to maintain the statistical structure of the atmosphere. In particular conservation of potential enstrophy, or enstrophy in barotropic non-divergent flows, not only prevents non-linear instability,

ARAKAWA (1966) and SADOURNY (1975a), but it is an essential feature of 2-dimensional barotropic flows and controls the exchanges of energy between different scales. Failure to conserve enstrophy in 2-dimensional non-divergent flows leads to a spurious computational cascade of energy to small scales resulting in an energy catastrophe, SADOURNY (1975a). The use of ad hoc lateral diffusion schemes can control the false numerical cascade by directly removing energy at the small scale end of the spectrum, but a false energy cascade into these scales in combination with excessive lateral smoothing, which is usually necessary to stabilize schemes with this defect, enhances the total amount of energy dissipation and removes erroneously energy from the weather bearing systems. It is therefore necessary to describe the dynamics of the truncated system (BASDEVANT and SADOURNY (1975)) as correctly as possible and to accurately describe the transfers of energy (and enstrophy) across the boundary imposed by truncation. An essential ingredient is conservation of enstrophy during vorticity advection by the non-divergent part of the wind.

The vertical co-ordinate is pressure normalised by the surface pressure, a sigma system, which allows exact satisfaction of the kinematic boundary condition at the surface of the earth. The model can be used with any specified irregular vertical resolution. We have chosen to use a regular spatially staggered latitude/longitude grid in the horizontal. The time-stepping algorithm is based on the explicit leap-frog scheme together with a spatial filtering technique to overcome the severe stability restriction arising from the convergence of the meridians to the poles.

In section 2 we describe the continuous equations for the model and in sections 3 and 4 the spatial and temporal differencing schemes are described.

In the last section, section 5, we present results of adiabatic integrations and also of some integrations with a dry convective adjustment scheme and a simple surface stress formulation.

2. The governing equations in sigma co-ordinates

The simplest sigma (σ) co-ordinate system has been chosen for the first version of the model, namely the system proposed by PHILLIPS (1957), in which

$$\sigma = p/p_s \tag{1}$$

where p is pressure and p_s is the pressure at the earth's surface. The sigma co-ordinate vertical velocity is

$$\dot{\sigma} = d\sigma/dt \tag{2}.$$

At the top of the model atmosphere ($\sigma=0$) we have set $\dot{\sigma}=0$ which gives the upper boundary condition

$$(p_s\dot{\sigma})_{\sigma=0} = 0. \tag{3}.$$

At the surface of the earth ($\sigma=1$) we have the kinematic boundary condition

$$(p_s\dot{\sigma})_{\sigma=1} = 0. \tag{4}.$$

Assuming the model atmosphere to be a perfect gas the hydrostatic equation can be expressed as

$$\frac{\partial \phi}{\partial \ell n \sigma} = - RT \tag{5}$$

where R is the gas constant, which for the purpose of this paper takes the value for dry air. A list of the variables and constants used in this paper is given in Table 1. The mass continuity equation (note the density in this sigma system is proportional to p_s) is

$$\frac{\partial p_s}{\partial t} + \frac{1}{a\cos(\theta)}\left\{ \frac{\partial}{\partial \lambda}(p_s u) + \frac{\partial}{\partial \theta}(p_s v\cos(\theta))\right\} + \frac{\partial}{\partial \sigma}(p_s\dot{\sigma}) = 0 \tag{6}.$$

This continuity equation is used to determine both $p_s\dot{\sigma}$ and $\frac{\partial p_s}{\partial t}$. Integrating equation (6) with respect to σ from $\sigma=0$ to σ

and using the upper boundary condition (3) we obtain

$$\sigma \frac{\partial p_s}{\partial t} + p_s\dot{\sigma} = -\int_0^{\sigma} \frac{1}{a\cos(\theta)}\left\{\frac{\partial}{\partial \lambda}(p_s u) + \frac{\partial}{\partial \theta}(p_s v\cos(\theta))\right\} d\sigma \tag{7}.$$

On setting $\sigma = 1$ in (7) and using the kinematic boundary condition (4) we obtain the pressure tendency equation

$$\frac{\partial p_s}{\partial t} = -\int_0^1 \frac{1}{a\cos(\theta)}\left\{\frac{\partial}{\partial\lambda}(p_s u) + \frac{\partial}{\partial\theta}(p_s v\cos(\theta))\right\}d\sigma \qquad (8)$$

$p_s\dot{\sigma}$ can now be determined from (7) and (8) by eliminating $\partial p_s/\partial t$. The zonal and meridional components of the momentum equations may be written

$$\frac{\partial u}{\partial t} - \frac{1}{\cos(\theta)} Z p_s v\cos(\theta) + \frac{1}{a\cos(\theta)}\frac{\partial}{\partial\lambda}(\phi+E) + RT\frac{1}{a\cos(\theta)}\frac{\partial}{\partial\lambda}(\ell n p_s) + \dot{\sigma}\frac{\partial u}{\partial\sigma} = F_u \qquad (9)$$

and

$$\frac{\partial v}{\partial t} + Z p_s u + \frac{1}{a}\frac{\partial}{\partial\theta}(\phi+E) + RT\frac{1}{a}\frac{\partial}{\partial\theta}(\ell n p_s) + \dot{\sigma}\frac{\partial v}{\partial\sigma} = F_v \qquad (10)$$

where Z is the potential absolute vorticity defined by

$$Z = \frac{1}{p_s}\left\{f + \frac{1}{a\cos(\theta)}\left(\frac{\partial v}{\partial\lambda} - \frac{\partial}{\partial\theta}(u\cos(\theta))\right)\right\} \qquad (11)$$

and E is the kinetic energy per unit mass given by

$$E = \tfrac{1}{2}\left(u^2 + \frac{1}{\cos(\theta)}v^2\cos(\theta)\right) \qquad (12)$$

The forms of the non-adiabatic forcing on the right hand sides of equations (9) and (10), and other equations, are not given in this paper. The first law of thermodynamics can be written

$$\frac{\partial T}{\partial t} + \frac{1}{p_s}\left[\frac{1}{a\cos(\theta)}\left(p_s u\frac{\partial T}{\partial\lambda} + p_s v\cos(\theta)\frac{\partial T}{\partial\theta}\right) + p_s\dot{\sigma}\frac{\partial T}{\partial\sigma} - \frac{\kappa T\omega}{\sigma}\right] = Q \qquad (13)$$

where ω is the pressure vertical velocity defined by

$$\omega = \frac{dp}{dt} = \frac{d}{dt}(p_s\sigma) = p_s\dot{\sigma} + \sigma\left(\frac{\partial p_s}{\partial t} + \frac{1}{a\cos(\theta)}\left(u\frac{\partial p_s}{\partial\lambda} + v\cos(\theta)\frac{\partial p_s}{\partial\theta}\right)\right)$$

$$= p_s\dot{\sigma} + \sigma\frac{\partial p_s}{\partial t} + \frac{\sigma}{a\cos(\theta)}\left\{p_s u\frac{\partial}{\partial\lambda}(\ell n p_s) + p_s v\cos(\theta)\frac{\partial}{\partial\theta}(\ell n p_s)\right\} \qquad (14)$$

The continuity equation for water vapour is

$$\frac{\partial q}{\partial t} + \frac{1}{p_s}\left[\frac{1}{a\cos(\theta)}\left(p_s u \frac{\partial q}{\partial \lambda} + p_s v \cos(\theta) \frac{\partial q}{\partial \theta}\right) + p_s \dot{\sigma} \frac{\partial q}{\partial \sigma}\right] = S. \qquad (15)$$

When $\dot{\sigma}$, ω and the non-adiabatic terms are determined, equations (6), (7), (8), (9), (10), (13) and (15) can be solved for the time changes of p_s, u, v, T and q and a forecast can be made.

p	pressure
p_s	surface pressure
ϕ	geopotential (g x height)
T	temperature
u	longitudinal/zonal velocity
v	latitudinal/meridional velocity
q	humidity mixing ratio
$Z=\frac{1}{p_s}\{f+\frac{1}{a\cos(\theta)}(\frac{\partial v}{\partial \lambda}-\frac{\partial (u\cos(\theta))}{\partial \theta})\}$	potential absolute vorticity
$E=\frac{1}{2}(u^2+\frac{1}{\cos(\theta)}v^2\cos(\theta))$	kinetic energy/unit mass
$\dot{\sigma}=\frac{d\sigma}{dt}$	sigma vertical velocity
$\omega=\frac{dp}{dt}=\frac{d}{dt}(\sigma p_s)$	pressure vertical velocity
$\sigma=p/p_s$	vertical co-ordinate
λ	longitude
θ	latitude
$f = 2\,\Omega\sin(\theta)$	Coriolis parameter
F_u, F_r, Q, S	non-adiabatic effects - sources/sinks
ϕ_s	geopotential of the earth's surface
R	gas constant
$\kappa=R/C_p$	
C_p	specific heat at constant pressure
Ω	angular velocity of the earth
g	acceleration due to gravity
a	radius of the earth.

Table 1 : LIST OF VARIABLES AND CONSTANTS USED IN THE MODEL.

3. The spatial differencing scheme

The dependent variables are staggered in space but not in time; the distribution of variables is illustrated in figures 1a and 1b. The horizontal wind components, temperature and humidity mixing ratio are kept at the main levels, levels k, and the vertical velocity $\dot{\sigma}$ and geopotential ϕ are kept at levels $k+\frac{1}{2}$. The vertical spacing of the levels is arbitrary and may vary from one level to another, whereas we use a regular latitude/longitude co-ordinate system in the horizontal. The horizontal grid is the ARAKAWA C grid and has been used by ARAKAWA, see ARAKAWA and LAMB (1976), for general circulation experiments and in the British Meteorological Office, BURRIDGE (1975), for operational short range forecasting. This grid has good dispersion properties for inertia gravity waves, giving an accurate simulation of the geostrophic adjustment process. In addition the C grid avoids two grid-length computational noise in the terms governing the motion of pure gravity waves.

We define

$$\Delta\sigma_k = \sigma_{k+\frac{1}{2}} - \sigma_{k-\frac{1}{2}}, \tag{16}$$

then

$$\sum_{k=1}^{K} \Delta\sigma_k = 1, \tag{17}$$

where K is the number of main levels (temperature levels). The upper and lower boundary conditions become

$$(p_S\dot{\sigma})_{\frac{1}{2}} = 0 \tag{18}$$

and

$$(p_S\dot{\sigma})_{K+\frac{1}{2}} = 0 \tag{19}$$

The values of σ_K and $\sigma_{k+\frac{1}{2}}$ are not independently specified but are related through consistency relations arising from energy constraints imposed on the finite difference scheme. This point will be discussed towards the end of the section.

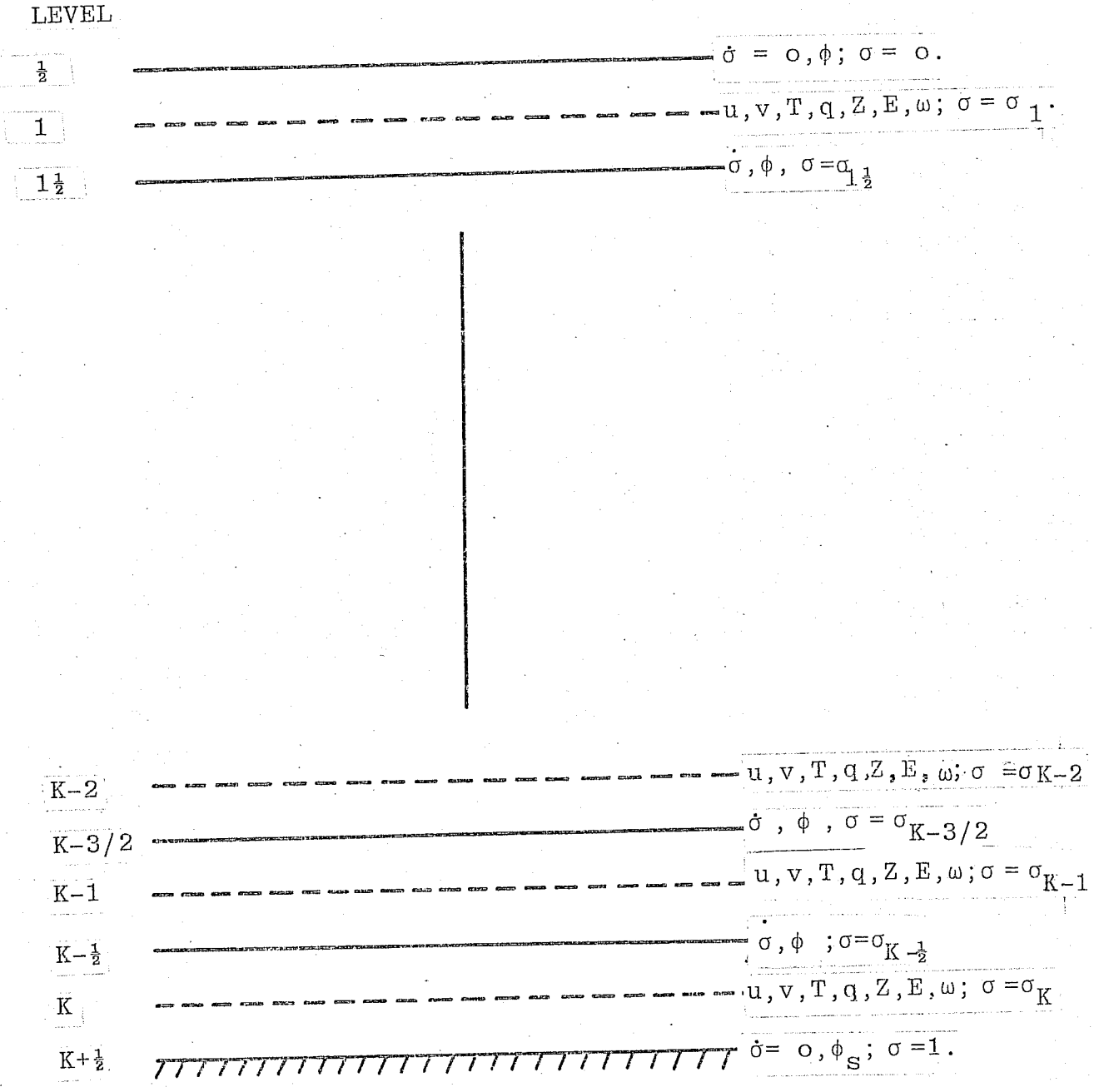

Figure 1a: Vertical distribution of variables.

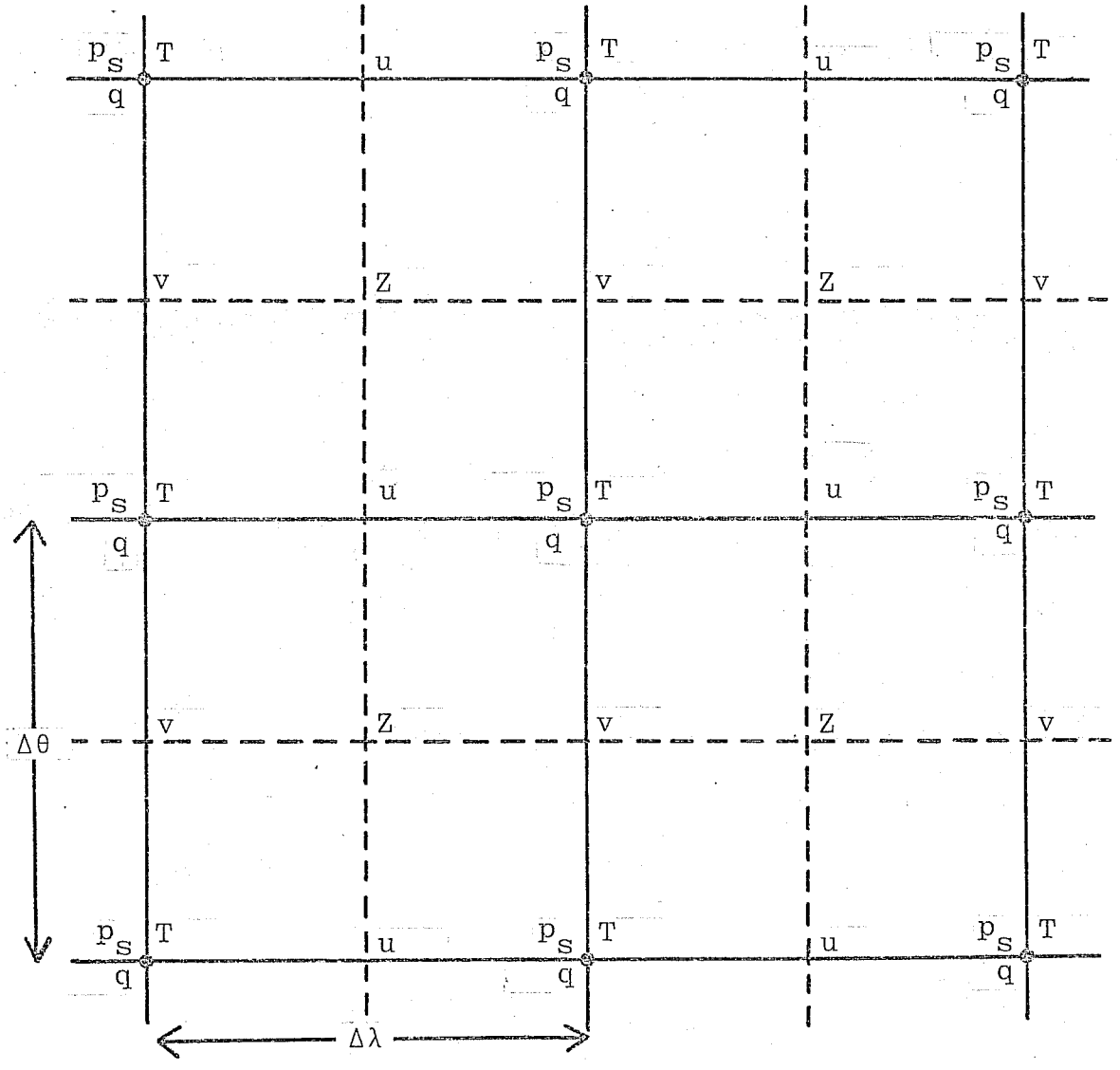

Figure 1b Horizontal distribution of variables.
(The variables E, ϕ, ω and $\dot{\sigma}$ are kept at temperature points).

In order to set down the finite difference scheme adopted, the following well known notation has been used :-

$$\overline{A}^{x}(x) = \tfrac{1}{2}\left(A(x+\tfrac{\Delta x}{2}) + A(x-\tfrac{\Delta x}{2})\right)$$

$$\overline{A}^{xy}(x,y) = \overline{A}^{x,y}(x,y) = \tfrac{1}{4}\left(A(x+\tfrac{\Delta x}{2}, y+\tfrac{\Delta y}{2}) + A(x-\tfrac{\Delta x}{2}, y+\tfrac{\Delta y}{2}) + A(x+\tfrac{\Delta x}{2}, y-\tfrac{\Delta y}{2}) + A(x-\tfrac{\Delta x}{2}, y-\tfrac{\Delta y}{2})\right)$$

$$\Delta_x A(x) = A(x+\tfrac{\Delta x}{2}) - A(x-\tfrac{\Delta x}{2})$$

$$\delta_x A(x) = \frac{\Delta_x A(x)}{\Delta x} \quad , \text{ for constant } \Delta x,$$

where Δx and Δy are grid lengths in the x and y directions respectively.

It is convenient to define 'mass flux' variables U and V by

$$\left.\begin{aligned} U &= \overline{p_s}^{\lambda} u \\ \text{and} \qquad & \\ V &= \overline{p_s}^{\theta} v \end{aligned}\right\} \qquad (20).$$

The hydrostatic equation is written

$$\frac{\Delta_\sigma \phi}{\Delta_\sigma \ell n \sigma} = -RT \qquad (21)$$

and a vertical summation of this equation gives

$$\phi_{k+\frac{1}{2}} = \phi_s + \sum_{\ell=k+1}^{K} RT_\ell (\Delta_\sigma \ell n \sigma)_\ell \qquad (22)$$

For the continuity equation and its vertically integrated forms, equations (6), (7) and (8), we have

$$\frac{\partial p_s}{\partial t} = \frac{1}{a\cos(\theta)} \left\{ \delta_\lambda U + \delta_\theta (V\cos(\theta)) \right\} + \frac{\Delta_\sigma (p_s \dot{\sigma})}{\Delta_\sigma \sigma} = 0 \qquad (23)$$

$$\sigma_{k+\frac{1}{2}} \frac{\partial p_s}{\partial t} + (p_s \dot{\sigma})_{k+\frac{1}{2}} = -\frac{1}{a\cos(\theta)} \sum_{\ell=1}^{K} \{\delta_\lambda U + \delta_\theta (V\cos(\theta))\}_\ell (\Delta_\sigma \sigma)_\ell \qquad (24)$$

and

$$\frac{\partial p_s}{\partial t} = -\frac{1}{a\cos(\theta)} \sum_{\ell=1}^{K} \{\delta_\lambda U + \delta_\theta (V\cos(\theta))\}_\ell (\Delta_\sigma \sigma)_\ell \qquad (25)$$

The special forms of all the finite difference equations for points in the neighbourhood of, and at, the poles are given separately at the end of this section. The global integral (finite difference sum) of the right hand side of equation (25) vanishes (with appropriate polar boundary conditions) ensuring exact conservation of the model's total mass. The momentum equations are differenced as (leaving the non-adiabatic terms in symbolic form)

$$\frac{\partial u}{\partial t} - \frac{1}{\cos(\theta)}\left[ZV\cos(\theta)\right] + \frac{1}{a\cos(\theta)}\delta_\lambda(\bar{\phi}^\sigma + E) + \frac{R\bar{T}^\lambda}{a\cos(\theta)}\delta_\lambda(\ell n p_s) + \frac{1}{\overline{p_s}^\lambda}\frac{\overline{\overline{p_s\dot{\sigma}}^\lambda \Delta_\sigma u}^\sigma}{\Delta_\sigma \sigma} = F_u \tag{26}$$

$$\frac{\partial v}{\partial t} + \left[ZU\right] + \frac{1}{a}\delta_\theta(\bar{\phi}^\sigma + E) + \frac{R\bar{T}^\theta}{a}\delta_\theta(\ell n p_s) + \frac{1}{\overline{p_s}^\theta}\frac{\overline{\overline{p_s\dot{\sigma}}^\theta \Delta_\sigma v}^\sigma}{\Delta_\sigma \sigma} = F_v \tag{27}$$

with

$$E = \tfrac{1}{2}\left(\overline{u^2}^\lambda + \frac{1}{\cos(\theta)}\overline{v^2\cos(\theta)}^\theta\right) \tag{28}$$

and

$$Z = \frac{1}{\overline{p_s}^{\lambda\theta}\, a\cos(\theta)}\left\{ f\cos(\theta) + \delta_\lambda v - \delta_\theta(u\cos(\theta))\right\} \tag{29}$$

We have chosen to work with two finite difference schemes for the rotation terms $\left[ZV\cos(\theta)\right]$ and $\left[Z\bar{U}\right]$. The first conserves both energy and potential absolute enstrophy, $(p_s Z^2)$, and for non-divergent barotropic flow may be reduced to the energy/enstrophy conserving Jacobian designed by ARAKAWA(1966). The second conserves potential absolute enstrophy $(p_s Z^2)$ but not energy. The energy/enstrophy conserving scheme we have chosen cannot easily be expressed in terms of the operators introduced above; instead we use a geometric description (SADOURNY 1975b) in which the rotation terms are written:

$$\left[ZV\cos(\theta)\right]_{oo} = \tfrac{1}{4}\Big[(V\cos(\theta))_{\frac{1}{2},\frac{1}{2}}(Z_{o,\frac{1}{2}}+Z_{o,-\frac{1}{2}}+Z_{1,\frac{1}{2}})/3$$

$$+(V\cos(\theta))_{-\frac{1}{2},\frac{1}{2}}\ (Z_{o,\frac{1}{2}}+Z_{o,-\frac{1}{2}}+Z_{-1,\frac{1}{2}})/3$$

$$+(V\cos(\theta))_{-\frac{1}{2},-\frac{1}{2}}(Z_{o,\frac{1}{2}}+Z_{o,-\frac{1}{2}}+Z_{-1,-\frac{1}{2}})/3$$

$$+(V\cos(\theta))_{\frac{1}{2},-\frac{1}{2}}\ (Z_{o,\frac{1}{2}}+Z_{o,-\frac{1}{2}}+Z_{1,-\frac{1}{2}})/3\ \Big]$$

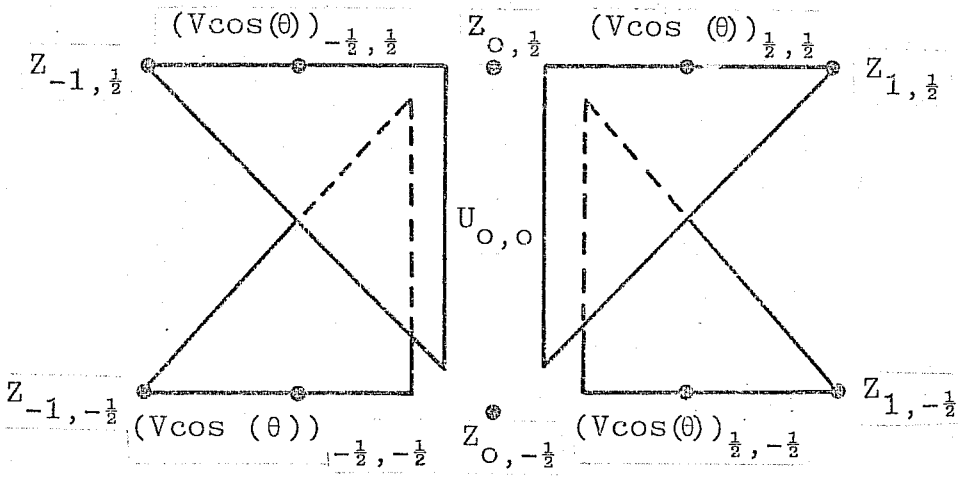

(30)

and

$$\begin{aligned}\left[ZU\right]_{o,o} = \tfrac{1}{4}\Big[& U_{\frac{1}{2},\frac{1}{2}}\,(Z_{-\frac{1}{2},o}+Z_{\frac{1}{2},o}+Z_{\frac{1}{2},1})/3 \\ & +U_{-\frac{1}{2},\frac{1}{2}}(Z_{-\frac{1}{2},o}+Z_{\frac{1}{2},o}+Z_{-\frac{1}{2},1})/3 \\ & +U_{-\frac{1}{2},-\frac{1}{2}}(Z_{-\frac{1}{2},o}+Z_{\frac{1}{2},o}+Z_{-\frac{1}{2},-1})/3 \\ & +U_{-\frac{1}{2},-\frac{1}{2}}(Z_{-\frac{1}{2},o}+Z_{\frac{1}{2},o}+Z_{-\frac{1}{2},-1})/3 \\ & +U_{\frac{1}{2},-\frac{1}{2}}(Z_{-\frac{1}{2},o}+Z_{\frac{1}{2},o}+Z_{\frac{1}{2},-1})/3 \Big] \end{aligned} \qquad (31)$$

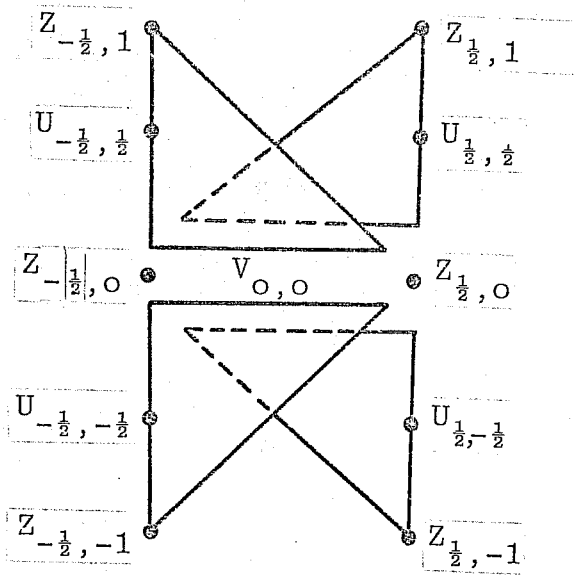

For the enstrophy conserving scheme we have chosen

$$\left[ZV\cos(\theta) \right] = \overline{V\cos(\theta)}^{xy}\ \overline{Z}^{y} \tag{32}$$

and

$$\left[ZU \right] = \overline{U}^{xy}\ \overline{Z}^{x} \tag{33}$$

The thermodynamic equation is used in the advective form

$$\frac{\partial T}{\partial t}+\frac{1}{p_s}\left\{\frac{1}{a\cos(\theta)}\left(\overline{U\delta_\lambda T}^{\lambda}+\overline{V\cos(\theta)\delta_\theta T}^{\theta}\right)+\frac{\overline{p_s\dot{\sigma}\ \Delta_\sigma T}^{\sigma}}{\Delta_\sigma \sigma}-\left[\frac{\kappa T\omega}{\sigma}\right]\right\}= Q \tag{34}$$

with

$$\left[\frac{\kappa T\omega}{\sigma}\right]= \frac{\kappa T}{\sigma}\left(\overline{\sigma\frac{\partial p_s}{\partial t}+p_s\dot{\sigma}}^{\sigma}\right)+\frac{\kappa}{a\cos(\theta)}\left\{\overline{U\overline{T}^{\lambda}\delta_\lambda(\ell n p_s)}^{\lambda}+\overline{V\cos(\theta)\overline{T}^{\theta}\delta_\theta(\ell n p_s)}^{\theta}\right\}. \tag{35}$$

Equation (34) may be rewritten in flux form using the finite difference continuity equation (23) and the finite difference rule

$$\Delta_x(A\overline{B}^{x}) = \overline{A\Delta_x B}^{x} + B\Delta_x A \tag{36}.$$

The form chosen for the ω term, relation (35), ensures that transformations between kinetic energy and total potential energy cancel provided $1/\sigma$ is defined by

$$\frac{1}{\sigma} = \frac{\Delta_\sigma \ell n\sigma}{\Delta_\sigma \sigma} \tag{37}$$

Equation (37) is the consistency requirement relating values of σ at temperature levels (levels k) to those at ($p_s\dot{\sigma}$) levels (levels $k+\frac{1}{2}$). A relation such as (37) is not strictly necessary for energy conservation since energy conservation is guaranteed when $\frac{\kappa T}{\sigma}$ in the first term on the right hand side of (35) is replaced by $-\frac{\kappa}{R}\frac{\Delta_\sigma \phi}{\Delta_\sigma \sigma}$, a finite difference representation for $-\frac{\kappa}{R}\frac{\partial \phi}{\partial \sigma}(=\frac{\kappa T}{\sigma})$, and in this case we have

$$\left[\frac{\kappa T_\omega}{\sigma}\right] = -\frac{1}{C_p}\frac{\Delta_\sigma \phi}{\Delta_\sigma \sigma}\left(\overline{\sigma\frac{\partial p_s}{\partial t}+ p_s\dot{\sigma}}^{\sigma}\right) + \frac{\kappa}{a\cos(\theta)}$$

$$\{\overline{U\bar{T}^{\lambda}}^{\lambda}\delta_\lambda(\ell n p_s) + \overline{V\cos(\theta)\bar{T}^{\theta}}^{\theta}\delta_\theta(\ell n p_s)\} \qquad (38)$$

Relation (35) subject to (37) is of this form.

The moisture equation is

$$\frac{\partial q}{\partial t} + \frac{1}{p_s}\left\{\frac{1}{a\cos(\theta)}\left[\overline{U\delta_\lambda q}^{\lambda} + \overline{V\cos(\theta)\delta_\theta q}^{\theta}\right] + \frac{\overline{p_s\dot{\sigma}\,\Delta_\sigma q}^{\sigma}}{\Delta_\sigma\sigma}\right\} = S \qquad (39)$$

which can be rewritten in a flux form and consequently moisture is conserved in the absence of sources and sinks.

3.1 Modification of the spatial differencing near and at the poles

We have chosen to keep temperatures at the poles as shown in figures 2a. and 2b. $P_s(=p_{s,p})$ at the poles changes as a result of the meridional mass flux $\bar{V}$ at all of the points on the latitude circle where the meridional velocity component v is carried. For the poles equation (23) is modified to give

$$\frac{\partial p_{s,p}}{\partial t} + (\text{SIGN})\frac{a\Delta\lambda}{\varepsilon}\sum_{i=1}^{IX}(V\cos(\theta))_{p-\frac{1}{2},i} + \frac{\Delta_\sigma(p_s\dot{\sigma})_p}{\Delta_\sigma\sigma} = 0 \qquad (40)$$

where IX is the number of points on a latitude circle,

$$\varepsilon = (IX)\left(\tfrac{1}{2}a\Delta\lambda\cos\left(\frac{\pi}{2} - \frac{\Delta\theta}{2}\right)\right)\left(\frac{a\Delta\theta}{2}\right) \qquad (41)$$

is the area represented by a polar grid point, and

$$\left.\begin{aligned}&\text{SIGN} = -1 \quad \text{for the North pole}\\ &\text{SIGN} = +1 \quad \text{for the South pole}\end{aligned}\right\} \qquad (42).$$

The polar surface pressure tendency $\frac{\partial p_s}{\partial t},p$ and vertical velocity $(p_s\dot{\sigma})_p$ can be determined from vertical integrals (finite difference sums) of (40), leading to the two equations

$$\sigma_{k+\frac{1}{2}}\frac{\partial p_{s,p}}{\partial t} + \left[(p_s\dot{\sigma})_p\right]_{k+\frac{1}{2}} = -\sum_{\ell=1}^{k}\left[(\text{SIGN})\frac{a\Delta\lambda}{\varepsilon}\sum_{i=1}(V\cos(\theta))_{p-\frac{1}{2},i}\right](\Delta_\sigma\sigma)_\ell \qquad (43)$$

and

$$\frac{\partial p_s}{\partial t}p = -\sum_{\ell=1}^{K}\left[(\text{SIGN})\frac{a\Delta\lambda}{\varepsilon}\sum_{i=1}^{IX}(V\cos(\theta))_{p-\frac{1}{2},i}\right](\Delta_\sigma\sigma)_\ell \qquad (44)$$

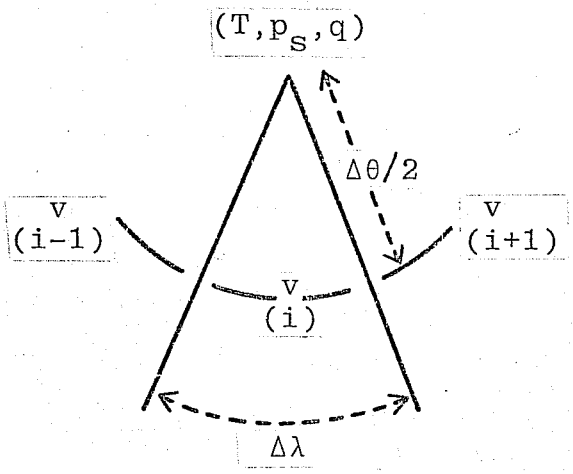

Figure 2a

Distribution of variables near and at the North pole.
(latitude / longitude grid).

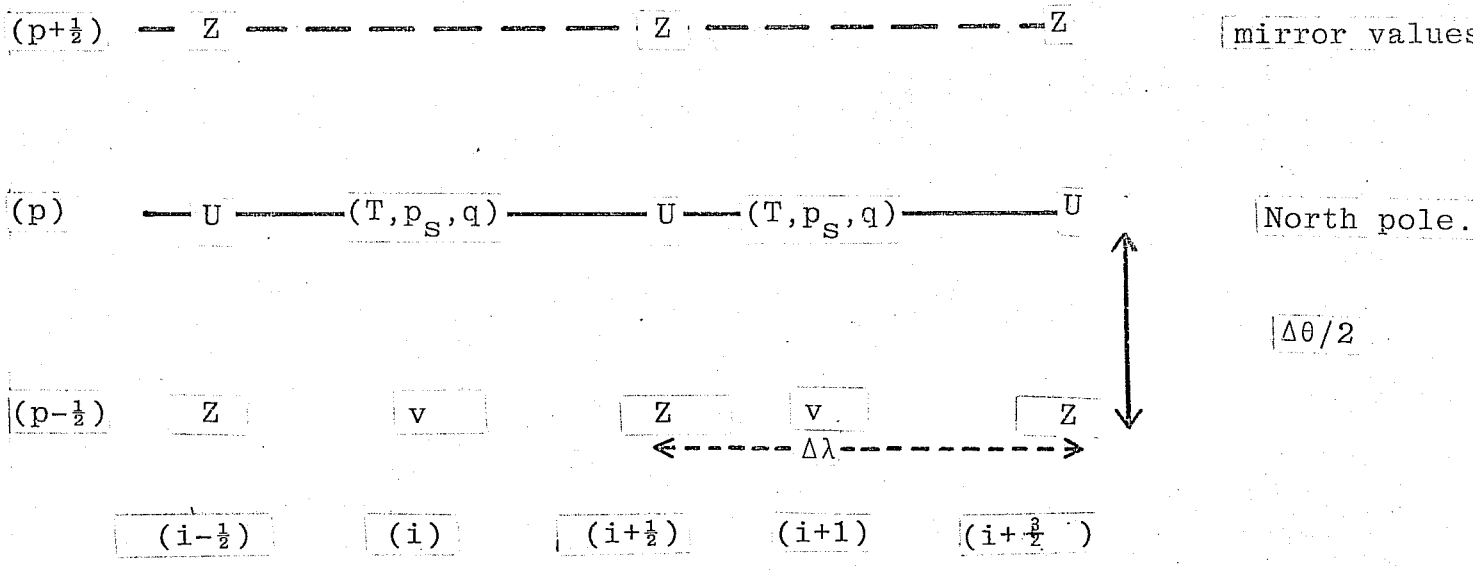

Figure 2b

Distribution of variables near and at the North pole.

The finite difference equation(27), the v equation, may be used to calculate $V_{p-\frac{1}{2},i}$ provided 'mirror values' $Z_{p+\frac{1}{2},i+\frac{1}{2}}$, the polar zonal mass flux, $U_{p,i}$ and kinetic energy /unit mass E_p are defined. We have chosen

$$Z_{p+\frac{1}{2},i+\frac{1}{2}} = Z_{p-\frac{1}{2},i+\frac{1}{2}} \tag{45}$$

and

$$E_p = \frac{1}{IX} \frac{1}{\frac{1}{2}\cos\left(\frac{\pi}{2} - \frac{\Delta\theta}{2}\right)} \sum_{i=1}^{IX} \frac{1}{2}(v_{p-\frac{1}{2},i})^2 \cos\left(\frac{\pi}{2} - \frac{\nabla\theta}{2}\right) \tag{46}$$

(NB. $\frac{1}{2}\cos\left(\frac{\pi}{2} - \frac{\Delta\theta}{2}\right)$ is the '$\cos(\theta)$' for the polar cap).

The zonal mass flux $U_{p,i}$ at the poles is not a true prognostic variable and is determined from finite difference representations of the polar boundary conditions

$$\left.\begin{aligned} &\frac{\partial U}{\partial \lambda} + \frac{\partial}{\partial \theta}(V\cos(\theta)) = \frac{1}{2\pi}\int_0^{2\pi} \frac{\partial}{\partial \theta}(V\cos(\theta))\, d\lambda \\ &\int_0^{2\pi} U d\lambda = 0 \end{aligned}\right\} \theta = \pm\frac{\pi}{2}, \tag{47}$$

which take the forms

$$\left(U_{p,i+\frac{1}{2}} - U_{p,i-\frac{1}{2}}\right)\frac{a\Delta\theta}{2} + (SIGN)V_{p-\frac{1}{2},i}\cos(\theta_{p-\frac{1}{2}})a\Delta\lambda =$$

$$= (SIGN)\frac{1}{IX}\sum_{i=1}^{IX} V_{p-\frac{1}{2},i}\cos(\theta_{p-\frac{1}{2}})\, a\Delta\lambda \tag{48}$$

and $$\sum_{i=1}^{IX} U_{p,i+\frac{1}{2}} = 0$$

respectively.

The choice of the mirror values of Z 'beyond' the poles (relation (45)) ensures conservation of potential absolute vorticity and potential absolute enstrophy by both forms chosen to represent the rotation terms, but energy conservation for the energy/enstrophy conserving scheme, (30) and (31), is limited by boundary effects at the poles resulting in boundary contributions from the rotation terms. These boundary terms are in fact very small and vanish for $Z_{p-\frac{1}{2},i+\frac{1}{2}}$ independent of i (Z constant on the boundary). If we let the poles be v points (Z points, with Z = constant on the boundaries) with v at the poles restricted to a zonal wave number one component and allow cross-polar differencing where necessary, the energy/enstrophy conserving scheme, (30)and (31), can be designed to be strictly energy and potential absolute enstrophy conserving.

The equations for T_p and q_p are

$$\frac{\partial T_p}{\partial t} + \frac{1}{p_s}\left\{(\text{SIGN})\,\frac{a\Delta\lambda}{\epsilon}\cos(\theta_{p-\frac{1}{2}})\sum_{i=1}^{IX}(V_{p-\frac{1}{2},i}\overline{T}^{\theta}_{p-\frac{1}{2},i}) + \overline{\frac{(p_s\dot{\sigma})_p\,\Delta_\sigma T_p}{\Delta_\sigma\sigma}}^{\sigma} - \left[\frac{\kappa T_\omega}{\sigma}\right]\right\} = Q_p \tag{49}$$

and

$$\frac{\partial q_p}{\partial t} + \frac{1}{p_s}\left\{(\text{SIGN})\,\frac{a\Delta\lambda}{\epsilon}\cos(\theta_{p-\frac{1}{2}})\sum_{i=1}^{IX}(V_{p-\frac{1}{2},i}\overline{q}^{\theta}_{p-\frac{1}{2},i}) + \overline{\frac{(p_s\dot{\sigma})_p\Delta_\sigma q_p}{\Delta_\sigma\sigma}}^{\sigma}\right\} = S_p \tag{50}$$

with

$$\left[\frac{\kappa T_\omega}{\sigma}\right]_p = -\frac{1}{C_p}\frac{\Delta_\sigma\phi_p}{\Delta_\sigma\sigma}\left(\sigma\overline{\frac{\partial p_s}{\partial t}+p_s\dot{\sigma}}^{\sigma}\right) + \frac{\kappa}{a\cos(\theta_{p-\frac{1}{2}})}\frac{1}{IX}\,x$$

$$x\sum_{i=1}^{IX}\overline{T}^{\theta}_{p-\frac{1}{2},i}V_{p-\frac{1}{2},i}\cos(\theta_{p-\frac{1}{2}})\;x\{\delta_\theta(\ell n p_s)\}_{p-\frac{1}{2},i} \tag{51}$$

with or without the constraint (37).

The basically second order centred spatial differencing scheme described in this section endows the model with the following properties, subject only to time truncation, non-adiabatic effects and boundary terms:-

(a) The total mass of the model is conserved.

(b) Kinetic energy (for scheme 31 and 32) p_sT^2, p_sq^2, moisture q and total potential energy are individually conserved under advective processes.

(c) Potential absolute enstrophy, p_sZ^2, and potential vorticity are conserved by the horizontal advection terms.

(d) The total energy is conserved with the correct conversion between kinetic and total potential energy.

4. The time-stepping scheme

Let $\underline{x}$ be a vector whose components are all the grid point values of the model's dependent variables, then we may formally write

$$\frac{\partial \underline{x}}{\partial t} + \underline{\underline{A}}\,\underline{x} + \underline{\underline{S}}\,\underline{x} = 0 \tag{52}$$

where $\underline{\underline{A}}$ and $\underline{\underline{S}}$ are non-linear finite difference operators representing the adiabatic terms in the governing equations (the terms set out in the last section) and the non-adiabatic terms respectively. Our present algorithm is based on a leap-frog scheme for the dynamics and a forward step for the remaining terms (some processes such as vertical diffusion may have to be included using implicit techniques to prevent numerical instability). The integration scheme is

$$\underline{x}\,(t+\Delta t) = \bar{\underline{x}}\,(t-\Delta t) - 2\Delta t\,\underline{\underline{A}}\,\underline{x}\,(t) - 2\Delta t\,\underline{\underline{S}}\,\underline{x}(t-\Delta t) \tag{53}$$

where the overbar denotes a linear time-filtering operator such that

$$\bar{\underline{x}}\,(t-\Delta t) = \underline{x}(t-\Delta t) + \alpha(\bar{\underline{x}}(t-2\Delta t) - 2x(t-\Delta t) + x(t)) \tag{54}$$

a typical value of α being 0.005. The properties of this filter are well known, ASSELIN (1972), and its purpose is to inhibit the growth of the spurious computational mode associated with the leap-frog scheme.

In order to overcome the severe stability restrictions arising from the convergence of the meridians to the poles, a latitudinally dependent spatial filtering operator, see ARAKAWA and LAMB (1976), is applied either selectively or to all the terms in the finite difference equations. Our filter can be formally expressed as the finite convolution operator

$$\underline{\underline{F}} = \underline{\underline{\Phi}}^{-1}\,\underline{\underline{\Lambda}}\,\underline{\underline{\Phi}} \tag{55}$$

where $\underline{\underline{\Phi}}$ is a finite Fourier transform along a line of latitude, Φ^{-1} its inverse and

$$\underline{\underline{\Lambda}} = \underline{\underline{\Lambda}}(\theta) = \mathrm{diag}(\Lambda_1(\theta)\ ,\text{----},\ \Lambda_N(\theta)\ ),$$

where $\Lambda_n(\theta)$ is the reduction factor for the n^{th} Fourier mode of the term being filtered. For linear systems this filter when applied to all terms (total tendency filtering) reduces the phase speeds of wave solutions of the equations. The filtering scheme has been designed so that the stability criterion for the finite difference scheme can be based on the east-west grid length at some fixed latitude, θ^{o} N, and the filter is then applied polewards of θ^{o} N and θ^{o} S in the Northern and Southern hemispheres respectively. Experiments with barotropic models using a number of filtering techniques will be described in another technical report.

5. Results

The integrations described in this section are based on initial data for 00 GMT 1st March 1965. The initial data set was constructed by interpolation from data on the GFDL N24 modified Kurihara grid, MIYAKODA (1974).
Our integrations which included topography were made with the global energy/enstrophy scheme, (30) and (31) with the following resolution:-

$$\Delta\lambda\left(\frac{180^o}{\pi}\right) = \Delta\theta\left(\frac{180^o}{\pi}\right) = \left(\frac{90^o}{24}\right) = 3.75^o \text{(approximately N24)}$$

nine temperature levels (the GFDL levels) with

$$\sigma_k = s_k^2\,(3-2s_k) \qquad k = 1,---,9$$

$$s_k = (2_{k-1})\,/18$$

and

$$\sigma_{k+\frac{1}{2}} = s_{k+\frac{1}{2}}^2\,(3-2s_{k+\frac{1}{2}}) \qquad k = 0,----,9$$

$$s_{k+\frac{1}{2}} = 2k/18$$

and with the relation (38) for $\left[\frac{\kappa T\omega}{\sigma}\right]$.

The time-step was 5 minutes and no time smoothing ($\alpha = 0$) or lateral diffusion was used. The spatial filter (53) was used for $/\theta\,(\frac{180^o}{\pi})/> 450$ with the reduction factors, ARAKAWA and LAMB (1976), defined as

$$\Lambda_n(\theta) = \frac{\cos(\theta^o)}{\cos(45^o)}\,\frac{1}{\sin\left[\frac{n\Delta\lambda}{2}\right]} \quad \text{if} \left(\frac{\cos(\theta^o)}{\cos(45^o)}\,\frac{1}{\sin\frac{n\Delta\lambda}{2}} < 1 \right)$$

$$= 1 \quad \text{if} \left(\frac{\cos(\theta^o)}{\cos(45^o)\sin\frac{n\Delta\lambda}{2}} \geqslant 1 \right)$$

The model's initial data is illustrated in figures (3) and (4) by 500 mb and 1000 mb. height charts; NMC analyses for this time are shown in figures (5) and (6). An adiabatic forecast to 72 hours together with NMC analyses are illustrated (500 mb and 1000 mb height charts) in figures (7) to (18).
It is not our intention to present a detailed analysis of the model's forecasting skill in this paper; its performance with the complete GFDL physical parameterisation scheme is demonstrated in a forthcoming technical report by GAUNTLETT et al (1977).
The general flow pattern of the 500 mb forecasts compares well

with the analyses though the intensities of the individual features are quite different. At 1000 mb the systems are much too intense, typical of integrations with no surface friction. The wind field at the lowest levels in the model grew rapidly (within the first 12 hours) to about twice the original values accompanied by the intensification of surface features. The energy loss in this adiabatic experiment was less than 5×10^{-7} % per time-step. By 72 hours many grid points, particularly over topography, have become seriously statically unstable and the integration became unstable before four days.

A 10 day forecast which included a simple frictional drag scheme at the surface of the earth and a dry convective adjustment scheme is illustrated in figures (19) to (24). The surface stress for this integration was

$$\underline{\tau} = C_D \left(|\overline{V}^{\lambda}| u, |\overline{V}^{\theta}| v \right)$$

with $$|V| = \sqrt{\overline{u^2}^{\lambda} + \frac{1}{\cos(\theta)} \overline{v^2 \cos\theta}^{\theta}}$$

and C_D (the non-dimensional drag coefficient) = 2×10^{-3}.

The major difference between the 72 hour forecasts, figures (11),(17),(20) and (23) is the large difference in the magnitude of the low level winds and the intensity of the surface features. The 10 day forecast has been included to demonstrate the stability of the model in the absence of ad hoc lateral smoothing schemes, though it is obvious from the 10 day 1000 mb chart, figure (24), there is a significant amount of noise at the limits of resolution of the model.

As mentioned above the next stage in the development of this model is to combine the adiabatic scheme of sections 3 and 4 with the GFDL physical parameterisation package and to evaluate its forecasting potential compared with that of other models available at ECMWF.

Acknowledgements

The authors thank the many members of the ECMWF Research Department who contributed constant encouragement and advice, in particular Dr. D. Gauntlett for many long and fruitful discussions.

The smooth development and flexibility of the programs owes a great deal to the valuable assistance provided by Mr. N. Storer and Mr. J. K. Gibson.

References

Arakawa, A. (1966) "Computational design for long term integrations of the equations of fluid motion", J.Comp.Phys., 1, pp.119-143.

Arakawa, A. and Lamb, V.R. (1976) "Computational design of the basic dynamical processes of the UCLA General Circulation Model", Dept.Meteorology University of California, Los Angeles.

Asselin, R. (1972) "Frequency filter for time integrations". Mon.Weath.Rev., 100, pp.487-490.

Basdevant, C. and Sadourny, R. (1975) "Ergodic properties of inviscid truncated models of two-dimensional incompressible flows", J.Fluid Mech.69, pp. 673-685.

Burridge, D.M. (1975) "A split semi-implicit reformulation of the Bushby-Timpson 10-level model", Quart.J.R.Met.Soc., 101, pp.777-792

Davies, H.C. (1976) "A lateral boundary formulation for multi-level prediction models", Quart.J.R.Met.Soc. 102, pp. 405-418

Gauntlett,D., Burridge, D.M.,and Arpe, K. (1977) in preparation

Källberg, P.	(1977)	" A test of a lateral boundary relaxation scheme in a barotropic model", ECMWF Internal Report No. 3, Research Dept.
Miyakoda, K.	(1974)	"GFDL Global 18-level atmospheric model using the modified Kurihara grid", Modelling for the first GARP Global Experiment GARP Publication
Phillips, N.A.	(1957)	"A co-ordinate system having some special advantages for numerical forecasting", J.Met., 14, pp. 184-185.
Sadourny, R.	(1975a)	"The dynamics of finite-difference models of the shallow-water equations", J.Atmos.Sci., 32, pp. 680-689.
Sadourny, R.	(1975b)	"Personal communication"

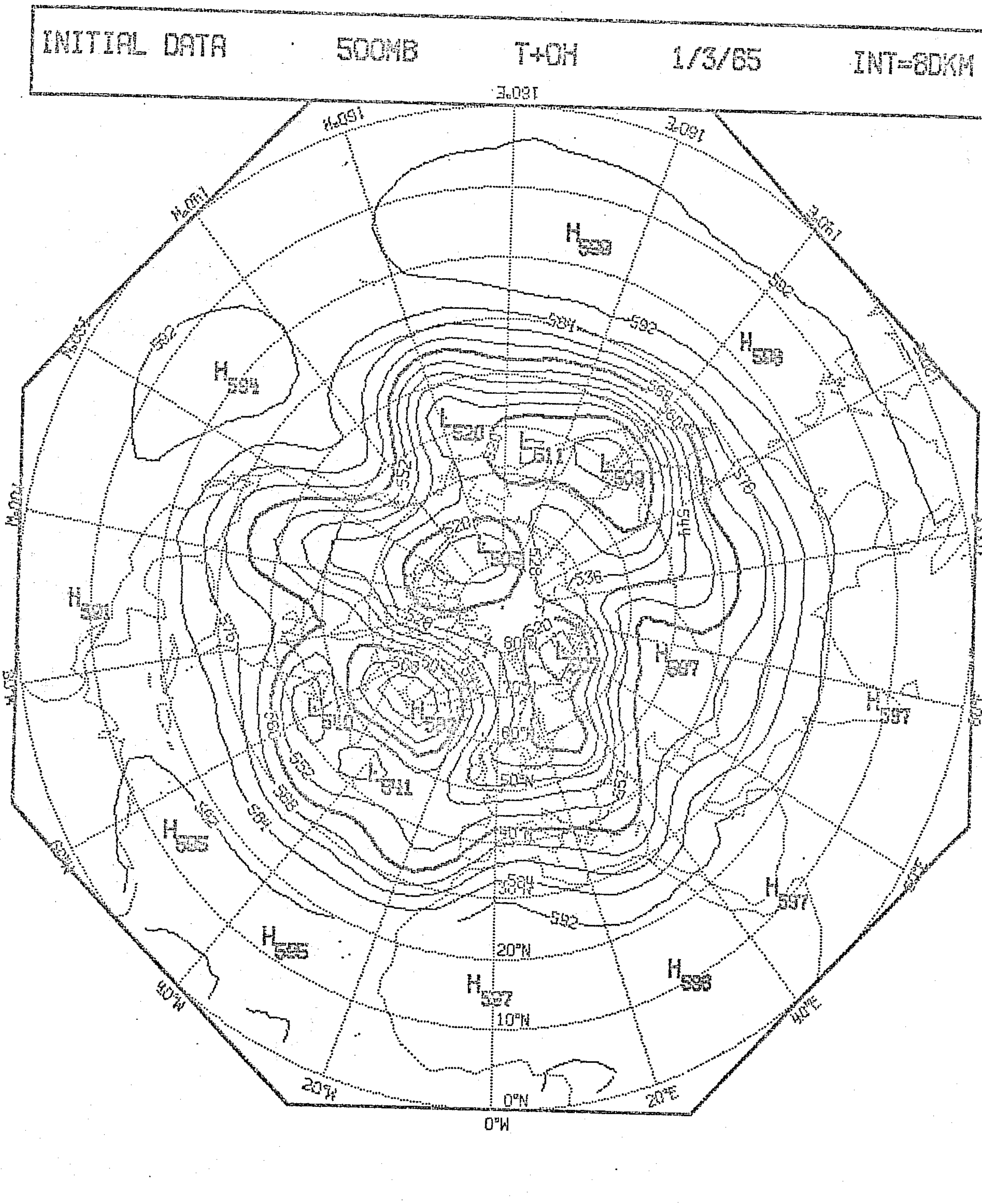
INITIAL DATA
500MB
T+0H
1/3/65
INT=8DKM
180°E
20°N
10°N
0°N
0°W
20°W
40°W
20°E
40°E

FIGURE 3

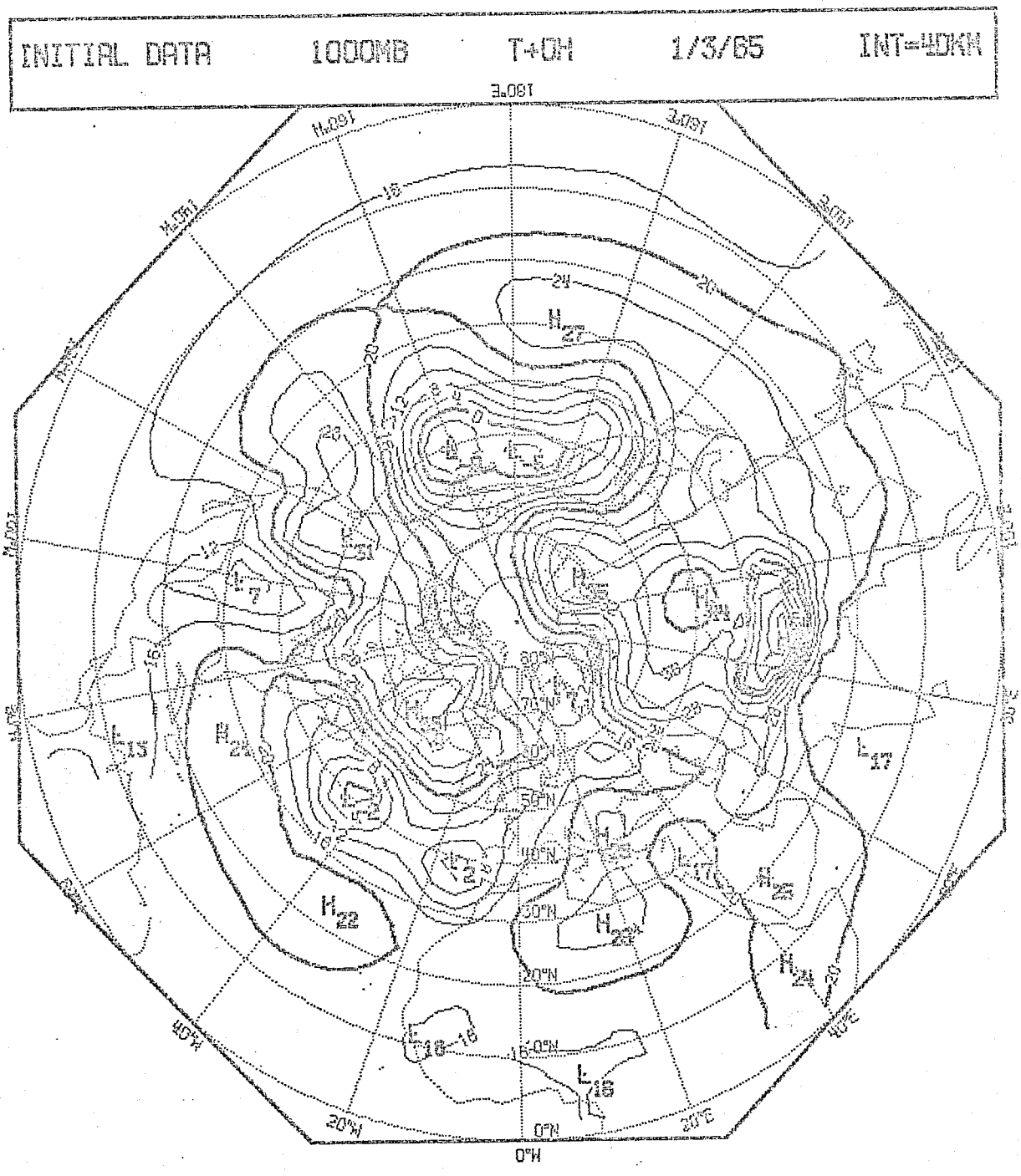
INITIAL DATA 1000MB T+0H 1/3/65 INT=40KM
180°E
0°W
0°N
20°N
40°N
60°N
80°N
20°E
40°E
60°E
80°E
100°E
120°E
140°E
160°E
160°W
140°W
120°W
100°W
80°W
60°W
40°W
20°W
H27
H24
H22
H25
H23
H21
L17
L16
L15
L18

FIGURE 4

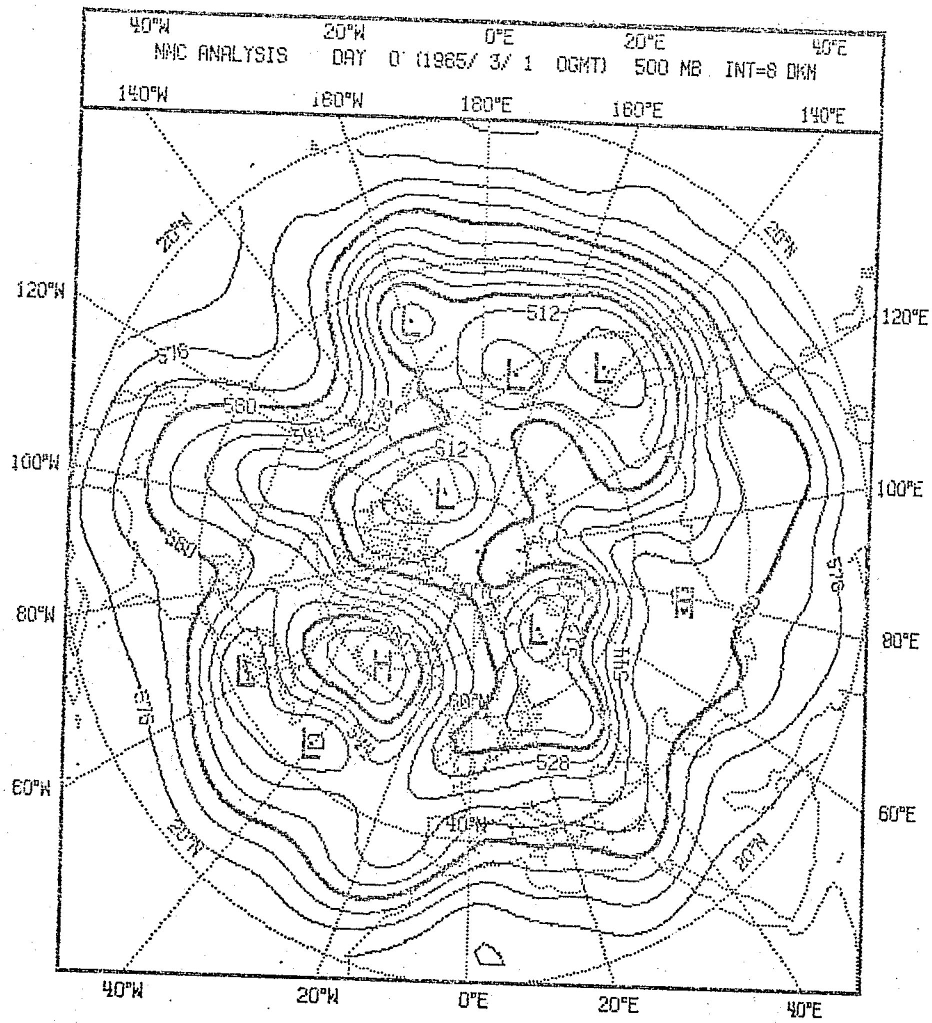
NMC ANALYSIS DAY 0 (1965/ 3/ 1 0GMT) 500 MB INT=8 DKM
40°W
20°W
0°E
20°E
40°E
140°W
160°W
180°E
160°E
140°E
120°W
100°W
80°W
60°W
120°E
100°E
80°E
60°E
20°N
40°N
60°N
512
528
576

FIGURE 5

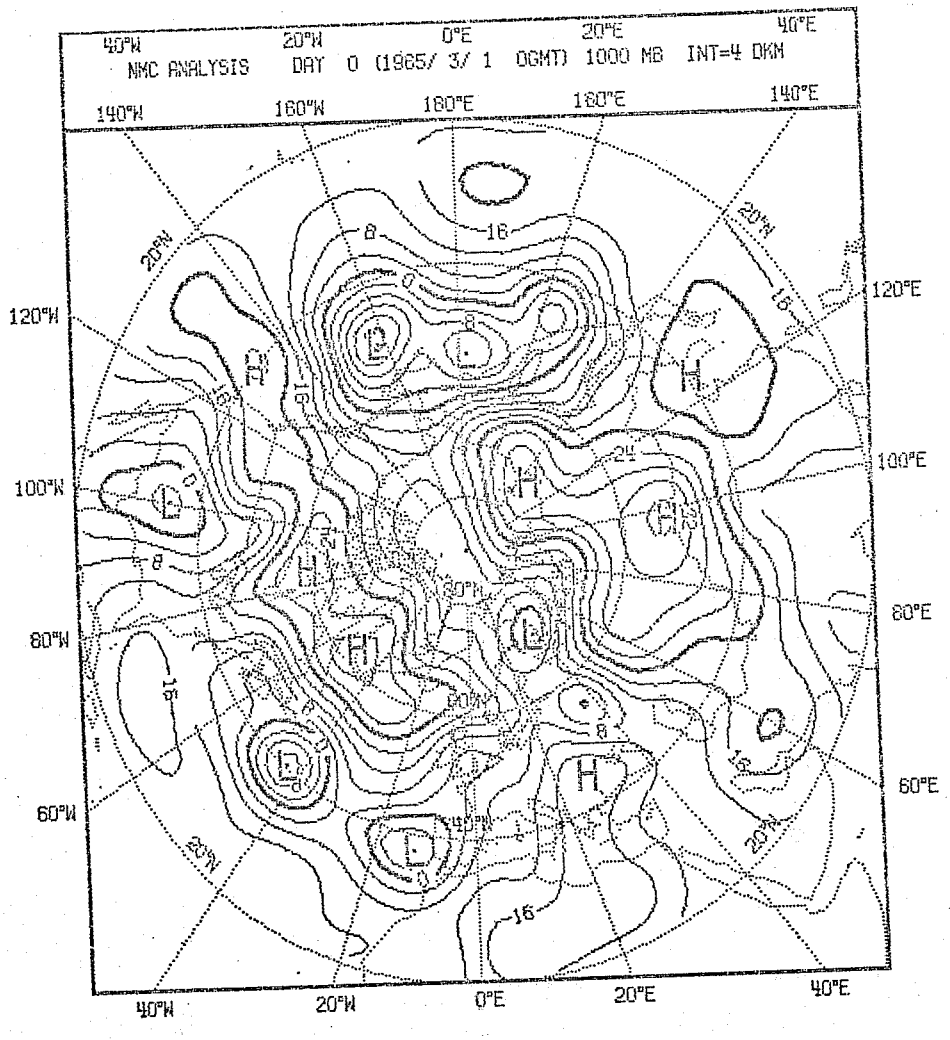
40°W 20°W 0°E 20°E 40°E
NMC ANALYSIS DAY 0 (1985/ 3/ 1 0GMT) 1000 MB INT=4 DKM
140°W 160°W 180°E 160°E 140°E
120°W 100°W 80°W 60°W
120°E 100°E 80°E 60°E
20°N
40°N
H
L
8
16
24
40°W 20°W 0°E 20°E 40°E

FIGURE 6

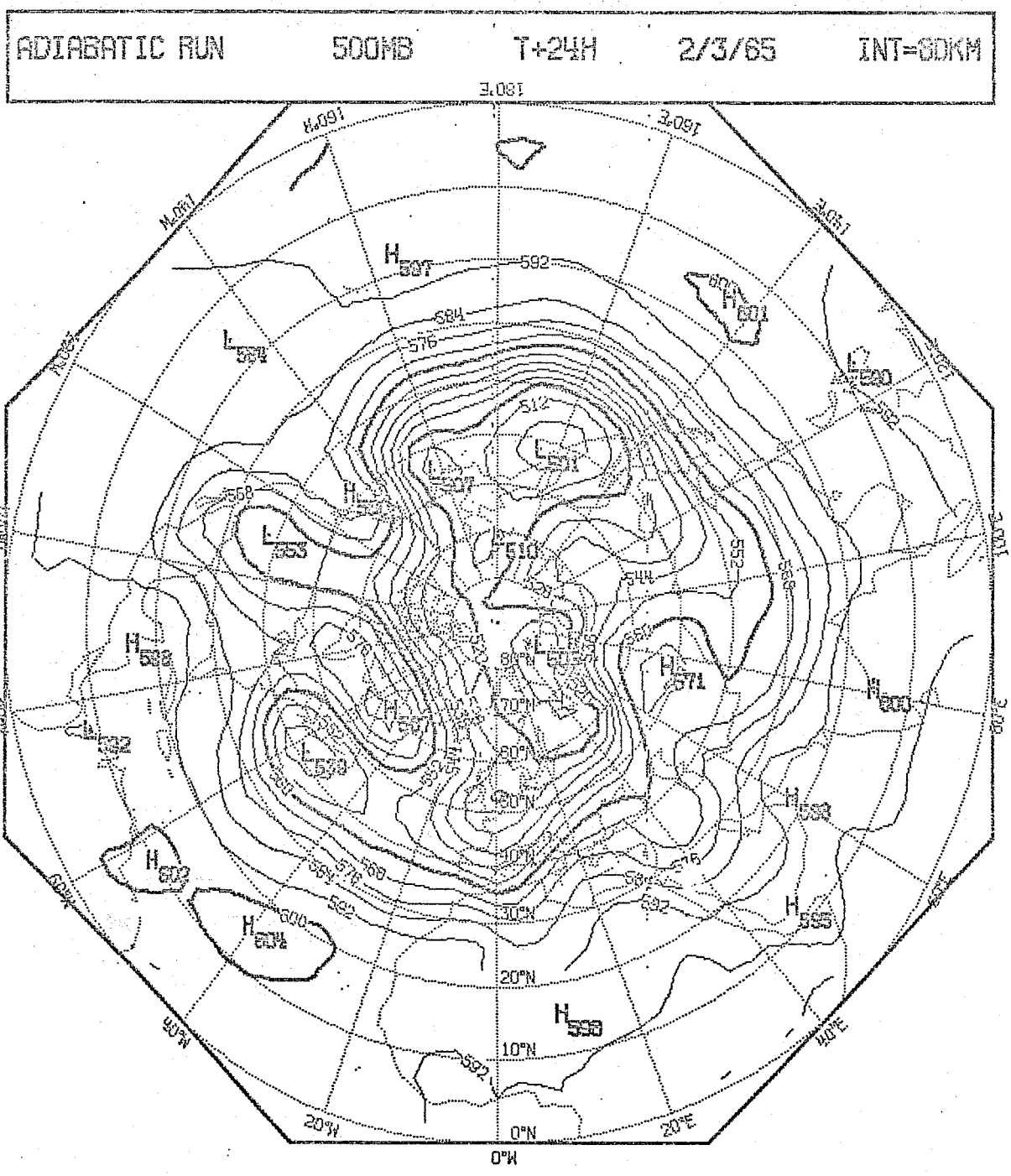
ADIABATIC RUN
500MB
T+24H
2/3/65
INT=60KM
180°E
160°W
140°W
120°W
100°W
80°W
60°W
40°W
20°W
0°W
20°E
40°E
60°E
80°E
100°E
120°E
140°E
160°E
180°E
80°N
70°N
60°N
50°N
40°N
30°N
20°N
10°N
0°N
H607
H601
H571
H568
H555
H558
H602
H598
H600
H592
L591
L590
L582
L580
L578
L576
L574
L573
L572
L571
L570
L569
L568
L567
L566
L565
L564
L563
L562
L561
L560
L559
L558
L557
L556
L555
L554
L553
L552
L551
L550
L549
L548
L547
L546
L545
L544
L543
L542
L541
L540
L539
L538
L537
L536
L535
L534
L533
L532
L531
L530
L529
L528
L527
L526
L525
L524
L523
L522
L521
L520
L519
L518
L517
L516
L515
L514
L513
L512
L511
L510
L509
L508
L507
L506
L505
L504
L503
L502
L501
L500
L499
L498
L497
L496
L495
L494
L493
L492
L491
L490
L489
L488
L487
L486
L485
L484
L483
L482
L481
L480
L479
L478
L477
L476
L475
L474
L473
L472
L471
L470
L469
L468
L467
L466
L465
L464
L463
L462
L461
L460
L459
L458
L457
L456
L455
L454
L453
L452
L451
L450
L449
L448
L447
L446
L445
L444
L443
L442
L441
L440
L439
L438
L437
L436
L435
L434
L433
L432
L431
L430
L429
L428
L427
L426
L425
L424
L423
L422
L421
L420
L419
L418
L417
L416
L415
L414
L413
L412
L411
L410
L409
L408
L407
L406
L405
L404
L403
L402
L401
L400
L399
L398
L397
L396
L395
L394
L393
L392
L391
L390
L389
L388
L387
L386
L385
L384
L383
L382
L381
L380
L379
L378
L377
L376
L375
L374
L373
L372
L371
L370
L369
L368
L367
L366
L365
L364
L363
L362
L361
L360
L359
L358
L357
L356
L355
L354
L353
L352
L351
L350
L349
L348
L347
L346
L345
L344
L343
L342
L341
L340
L339
L338
L337
L336
L335
L334
L333
L332
L331
L330
L329
L328
L327
L326
L325
L324
L323
L322
L321
L320
L319
L318
L317
L316
L315
L314
L313
L312
L311
L310
L309
L308
L307
L306
L305
L304
L303
L302
L301
L300
L299
L298
L297
L296
L295
L294
L293
L292
L291
L290
L289
L288
L287
L286
L285
L284
L283
L282
L281
L280
L279
L278
L277
L276
L275
L274
L273
L272
L271
L270
L269
L268
L267
L266
L265
L264
L263
L262
L261
L260
L259
L258
L257
L256
L255
L254
L253
L252
L251
L250
L249
L248
L247
L246
L245
L244
L243
L242
L241
L240
L239
L238
L237
L236
L235
L234
L233
L232
L231
L230
L229
L228
L227
L226
L225
L224
L223
L222
L221
L220
L219
L218
L217
L216
L215
L214
L213
L212
L211
L210
L209
L208
L207
L206
L205
L204
L203
L202
L201
L200
L199
L198
L197
L196
L195
L194
L193
L192
L191
L190
L189
L188
L187
L186
L185
L184
L183
L182
L181
L180
L179
L178
L177
L176
L175
L174
L173
L172
L171
L170
L169
L168
L167
L166
L165
L164
L163
L162
L161
L160
L159
L158
L157
L156
L155
L154
L153
L152
L151
L150
L149
L148
L147
L146
L145
L144
L143
L142
L141
L140
L139
L138
L137
L136
L135
L134
L133
L132
L131
L130
L129
L128
L127
L126
L125
L124
L123
L122
L121
L120
L119
L118
L117
L116
L115
L114
L113
L112
L111
L110
L109
L108
L107
L106
L105
L104
L103
L102
L101
L100
L99
L98
L97
L96
L95
L94
L93
L92
L91
L90
L89
L88
L87
L86
L85
L84
L83
L82
L81
L80
L79
L78
L77
L76
L75
L74
L73
L72
L71
L70
L69
L68
L67
L66
L65
L64
L63
L62
L61
L60
L59
L58
L57
L56
L55
L54
L53
L52
L51
L50
L49
L48
L47
L46
L45
L44
L43
L42
L41
L40
L39
L38
L37
L36
L35
L34
L33
L32
L31
L30
L29
L28
L27
L26
L25
L24
L23
L22
L21
L20
L19
L18
L17
L16
L15
L14
L13
L12
L11
L10
L9
L8
L7
L6
L5
L4
L3
L2
L1

FIGURE 7

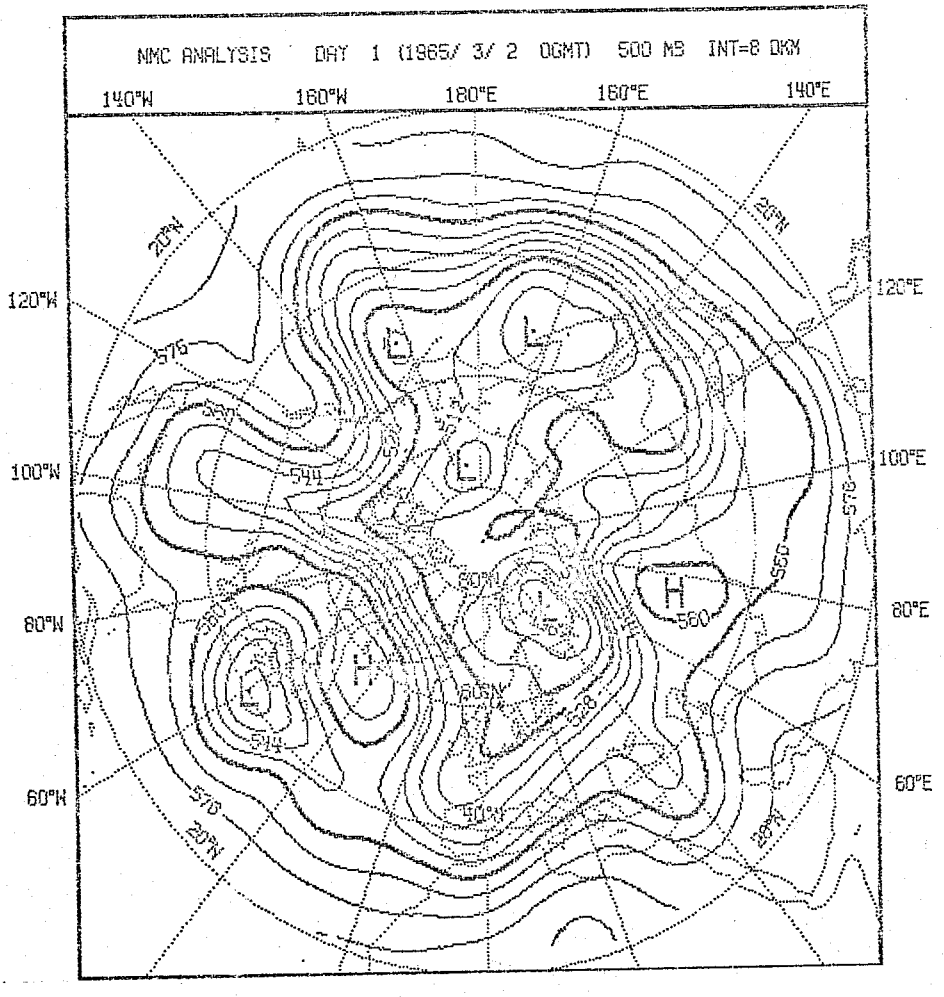
NMC ANALYSIS DAY 1 (1985/ 3/ 2 0GMT) 500 MB INT=8 DKM
140°W
160°W
180°E
160°E
140°E
120°W
120°E
100°W
100°E
80°W
80°E
60°W
60°E
20°N
50°N
H
560
L
544
576

FIGURE 8

ADIABATIC RUN 500MB T+48H 3/3/65 INT=8DKM

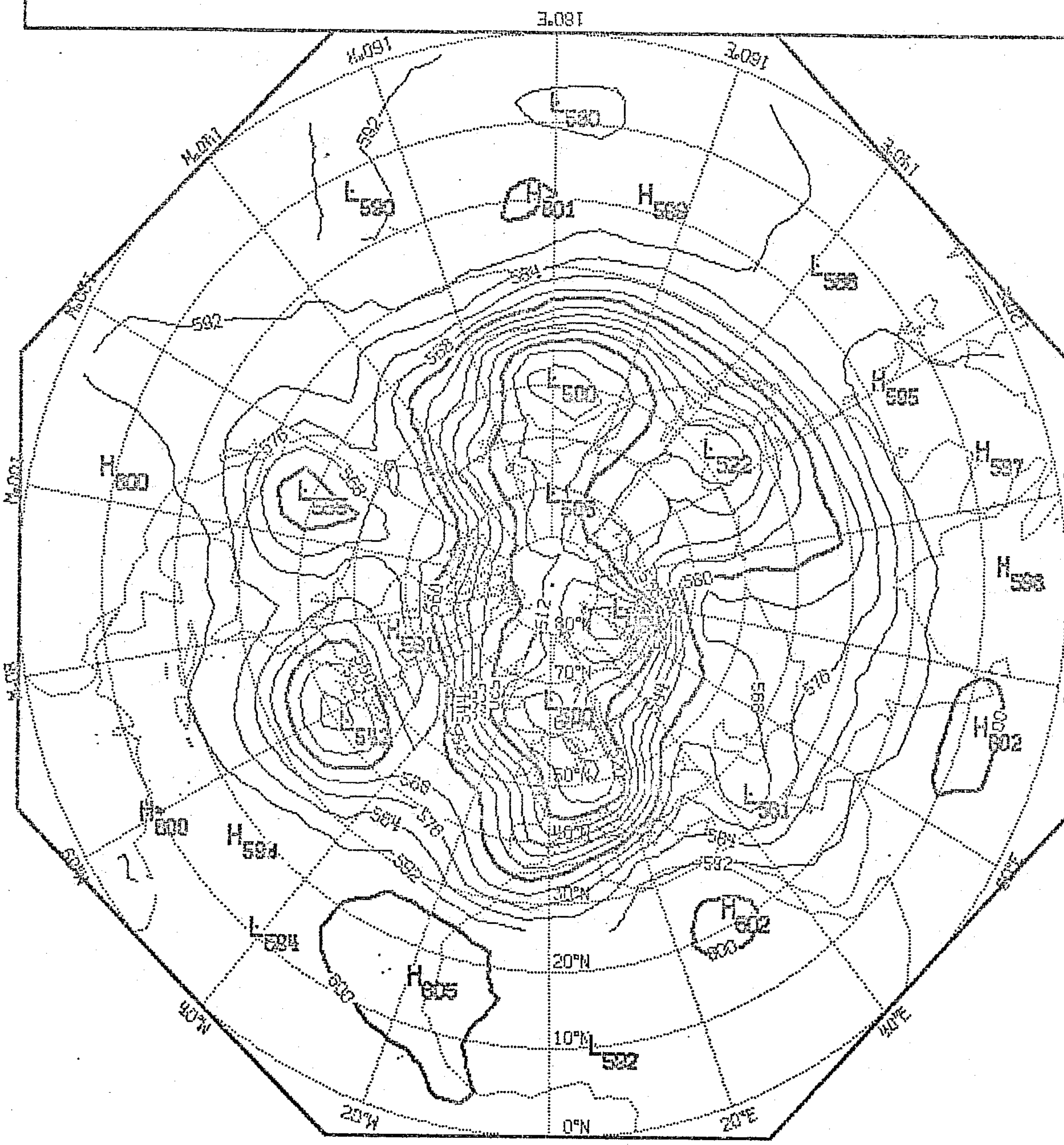

FIGURE 9

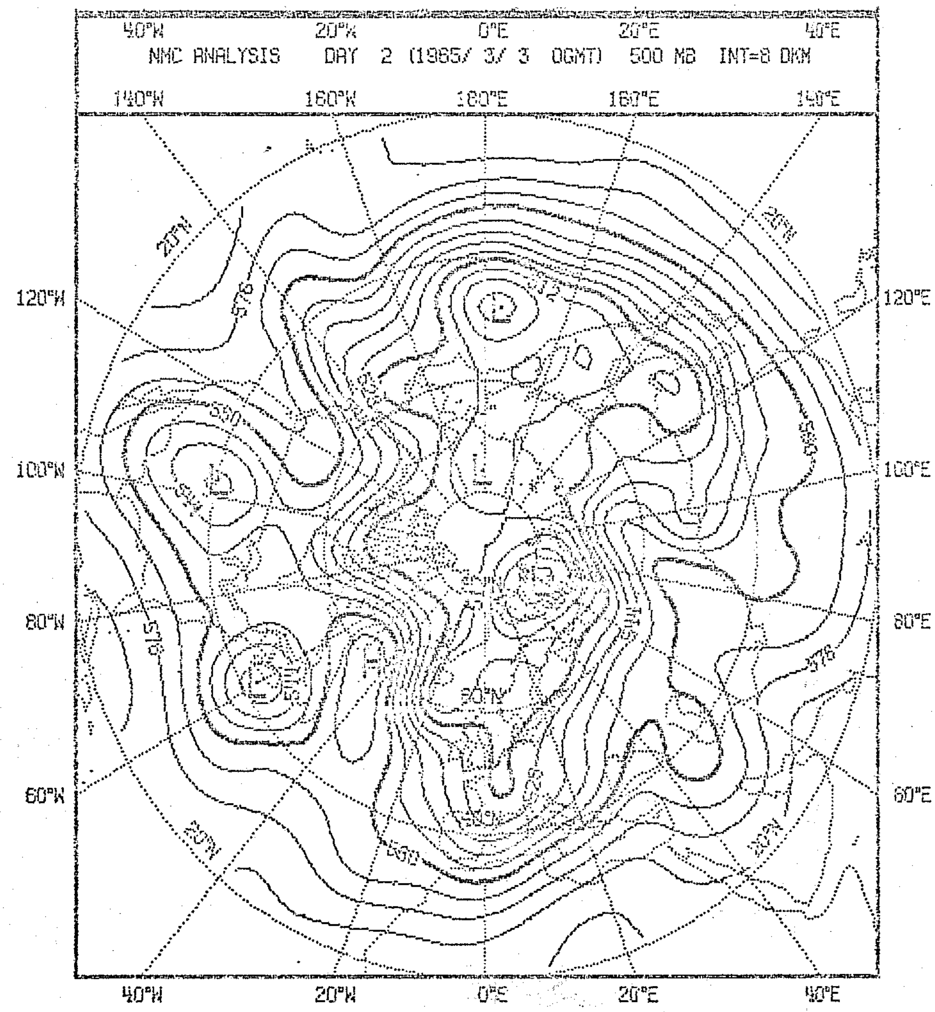
40°W
20°W
0°E
20°E
40°E
NMC ANALYSIS DAY 2 (1985/ 3/ 3 0GMT) 500 MB INT=8 DKM
140°W
160°W
180°E
160°E
140°E
120°W
120°E
100°W
100°E
80°W
80°E
60°W
60°E
576
550
560
90°N
20°N

FIGURE 10

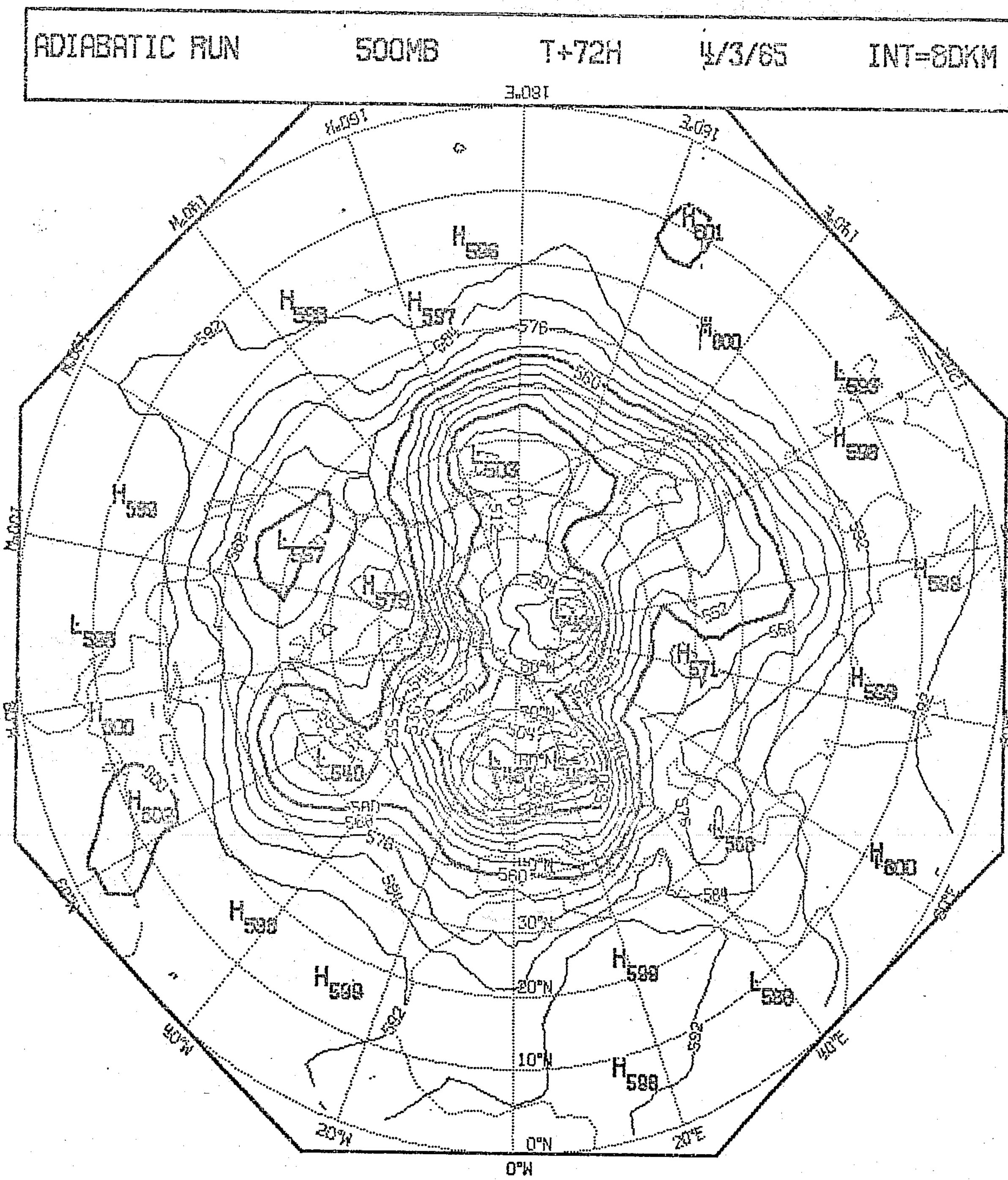
ADIABATIC RUN
500MB
T+72H
4/3/65
INT=8DKM
180°E
0°N
0°W
10°N
20°N
30°N
40°E
20°E
20°W
40°W

FIGURE 11

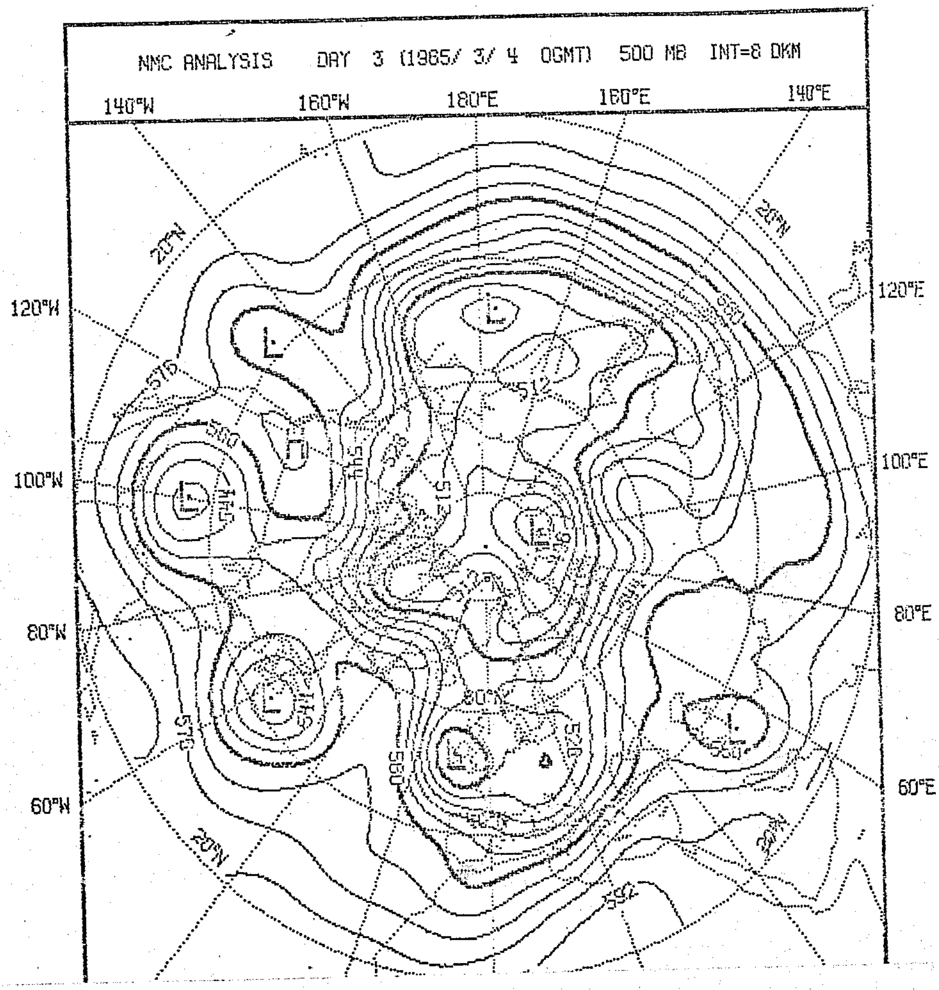
NMC ANALYSIS DAY 3 (1965/ 3/ 4 0GMT) 500 MB INT=8 DKM
140°W
160°W
180°E
160°E
140°E
120°W
100°W
80°W
60°W
120°E
100°E
80°E
60°E
20°N
20°N
20°N
20°N
80°N
576
560
544
528
512
520
552
L

FIGURE 12

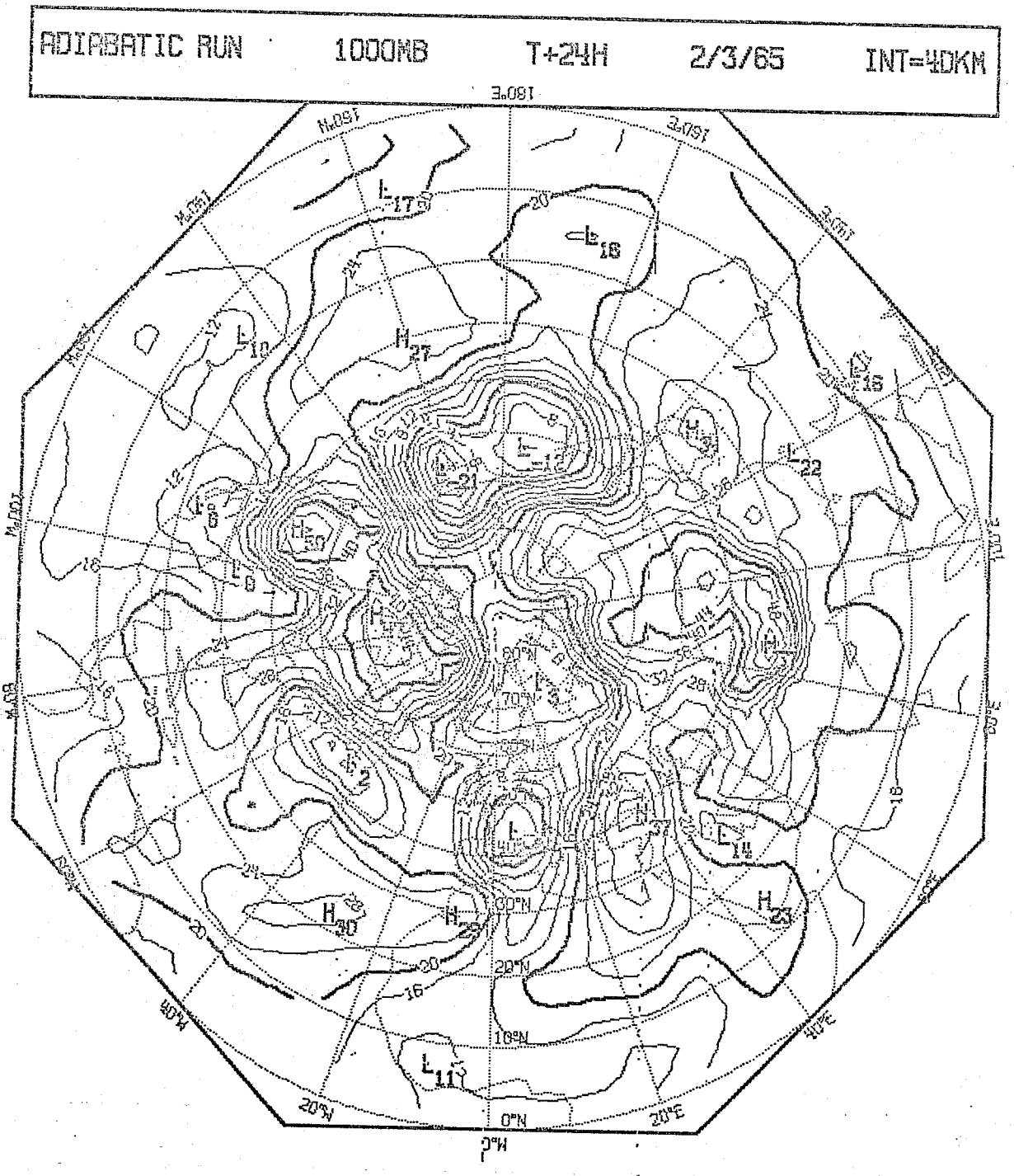
ADIABATIC RUN
1000MB
T+24H
2/3/65
INT=40KM
180°E
160°W
140°W
120°W
100°W
80°W
60°W
40°W
20°W
0°W
20°E
40°E
60°E
80°E
100°E
120°E
140°E
160°E
180°E
80°N
70°N
60°N
50°N
40°N
30°N
20°N
10°N
0°N
L17
L18
L10
H27
L15
L22
L6
L9
H30
H29
H23
L14
L11
H25
L12
L21

FIGURE 13

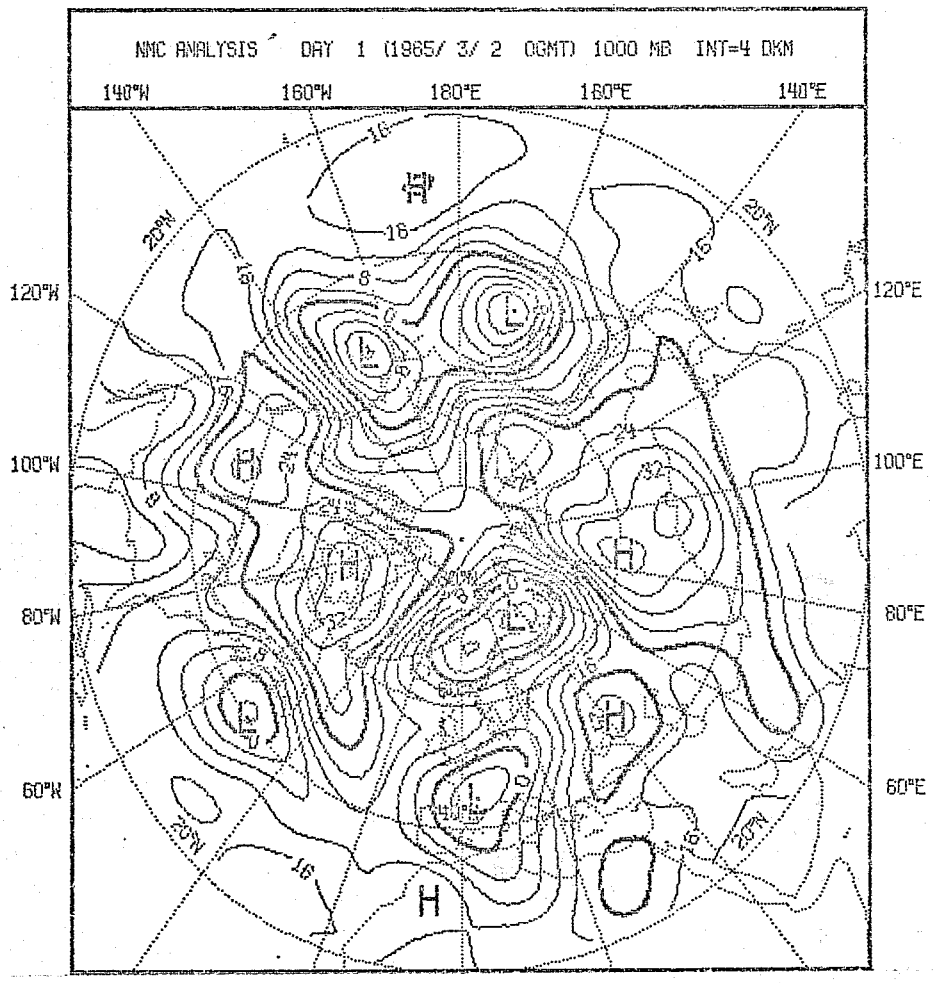
NMC ANALYSIS DAY 1 (1985/ 3/ 2 00GMT) 1000 MB INT=4 DKM
140°W
160°W
180°E
160°E
140°E
120°W
100°W
80°W
60°W
120°E
100°E
80°E
60°E
20°N
16
8
H
L

FIGURE 14

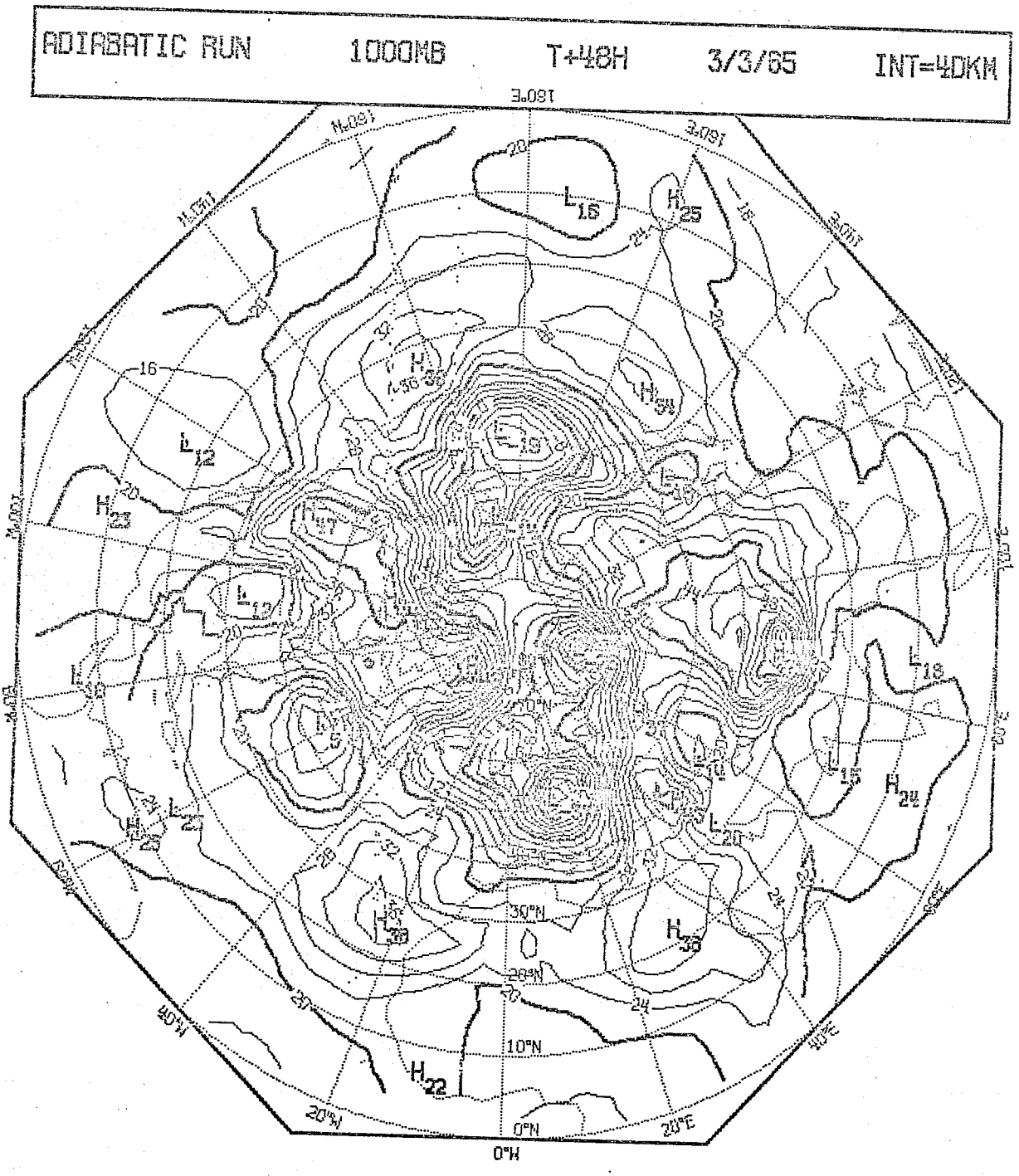
ADIABATIC RUN
1000MB
T+48H
3/3/65
INT=40KM
180°E
160°W
140°W
120°W
100°W
80°W
60°W
40°W
20°W
0°W
20°E
40°E
60°E
80°E
100°E
120°E
140°E
160°E
180°E
70°N
50°N
30°N
10°N
0°N
L15
H25
H35
H34
L19
L12
H23
L17
L13
L18
L15
H24
H25
L20
H35
L35
H22

FIGURE 15

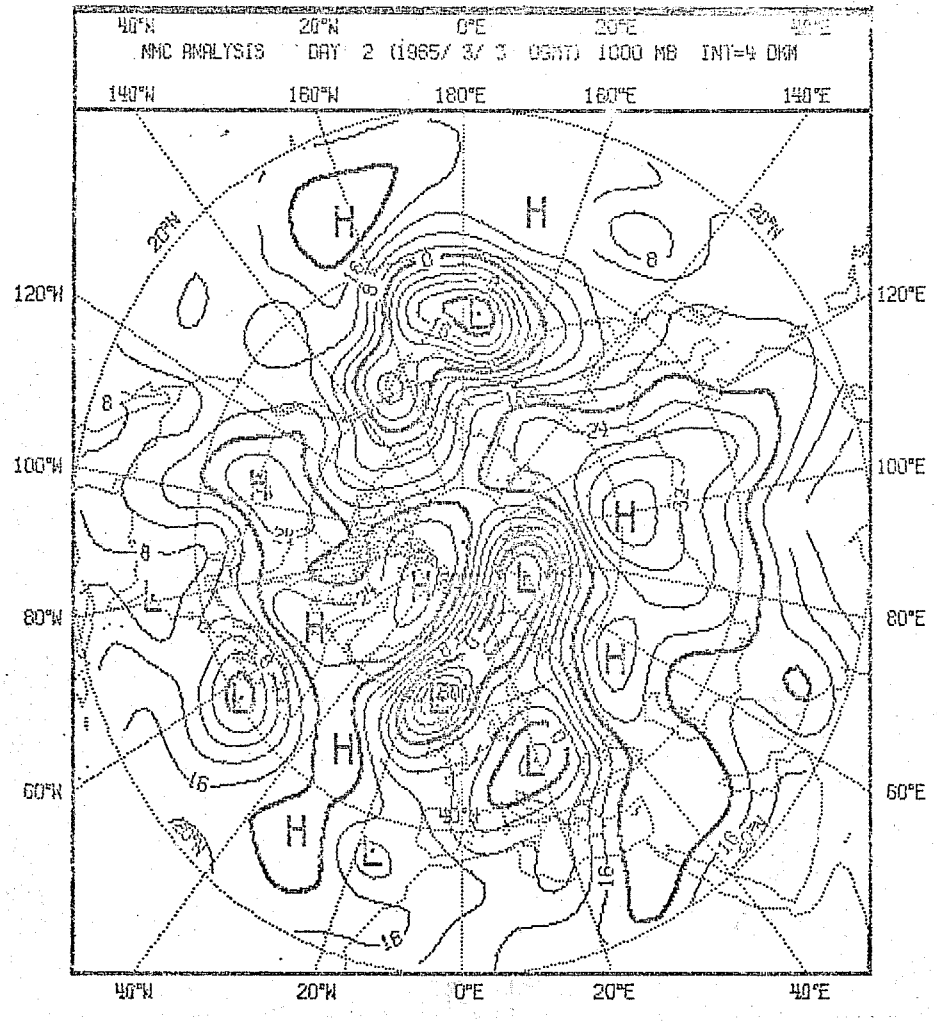
40°W
20°W
0°E
20°E
40°E
NMC ANALYSIS DAY 2 (1985/ 3/ 3 0GMT) 1000 MB INT=4 DAM
140°W
180°W
180°E
140°E
120°W
120°E
100°W
100°E
80°W
80°E
60°W
60°E
20°N
H
L

FIGURE 16

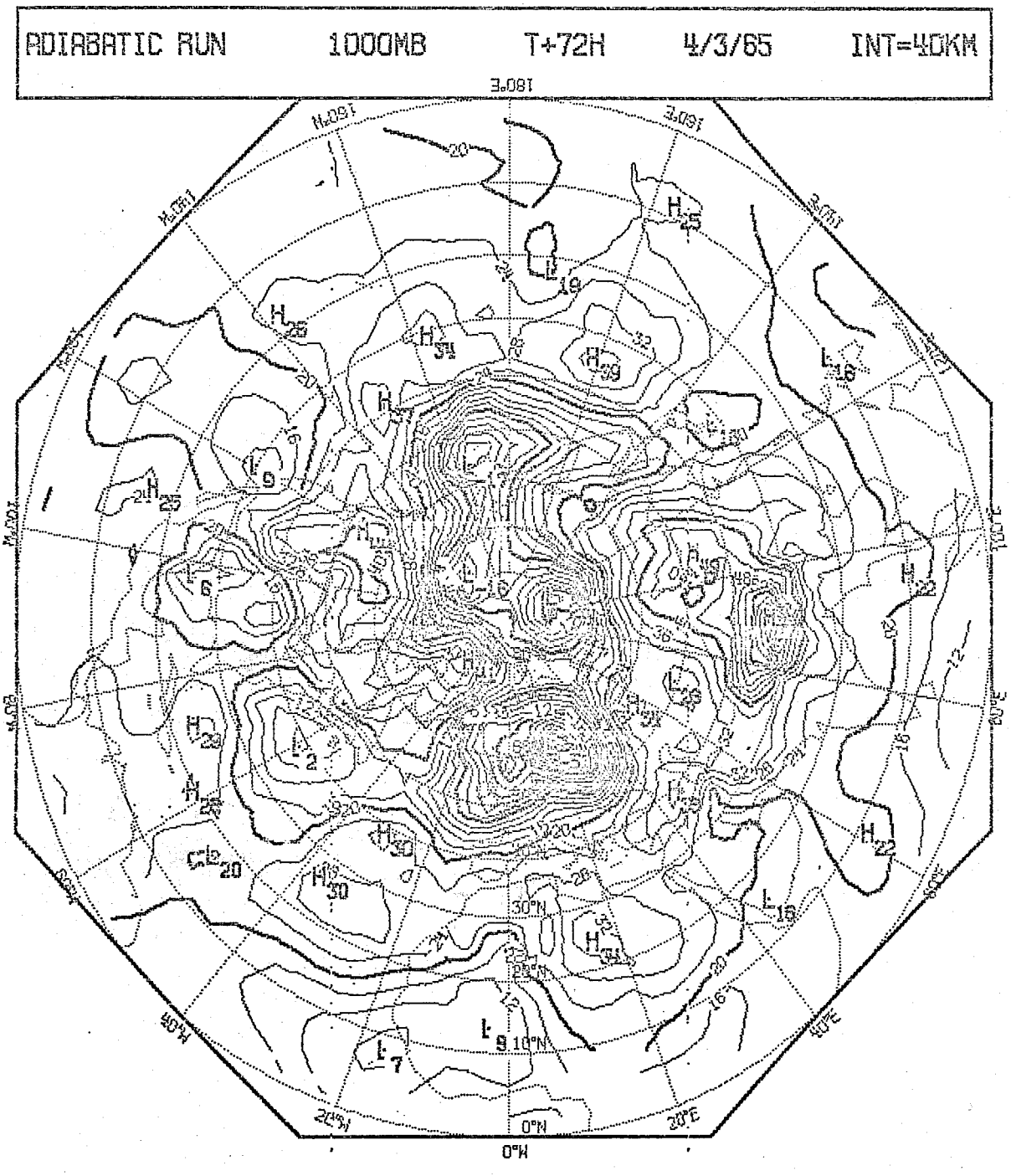

FIGURE 17

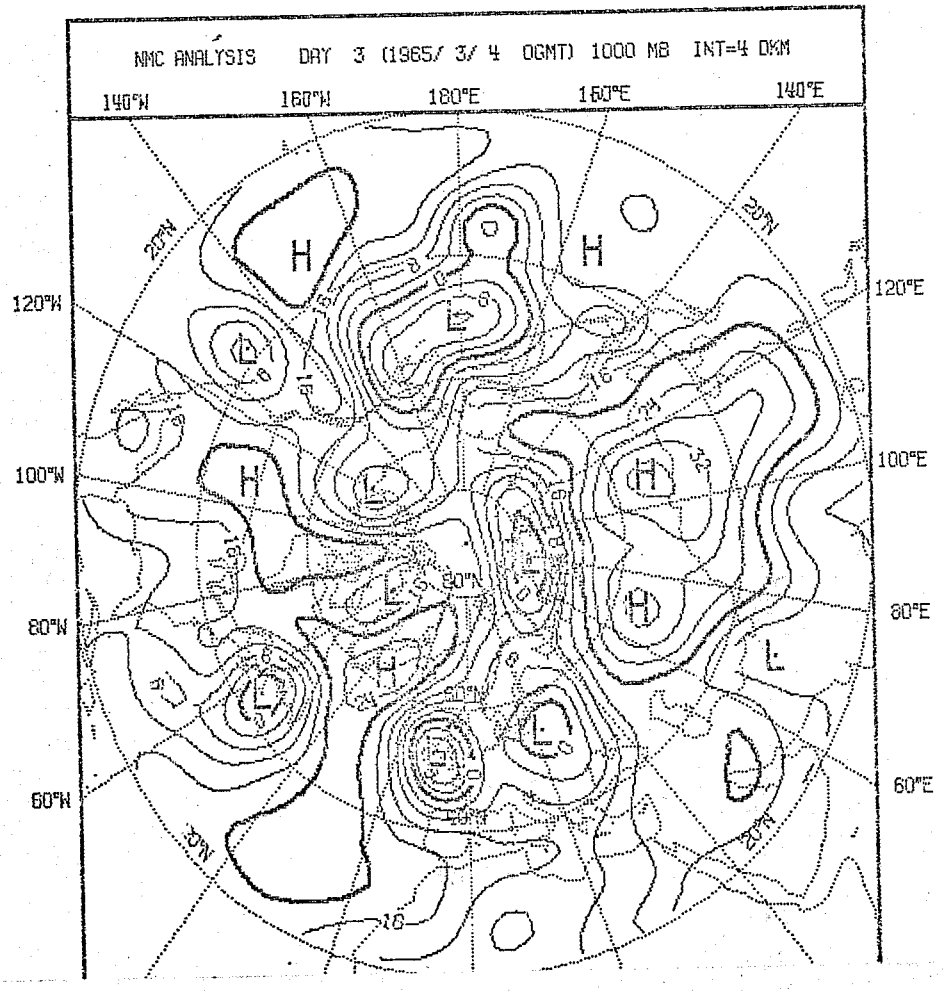
NMC ANALYSIS DAY 3 (1985/ 3/ 4 0GMT) 1000 MB INT=4 DAM
140°W
160°W
180°E
160°E
140°E
120°W
100°W
80°W
60°W
120°E
100°E
80°E
60°E
80°N
20°N
H
L

FIGURE 18

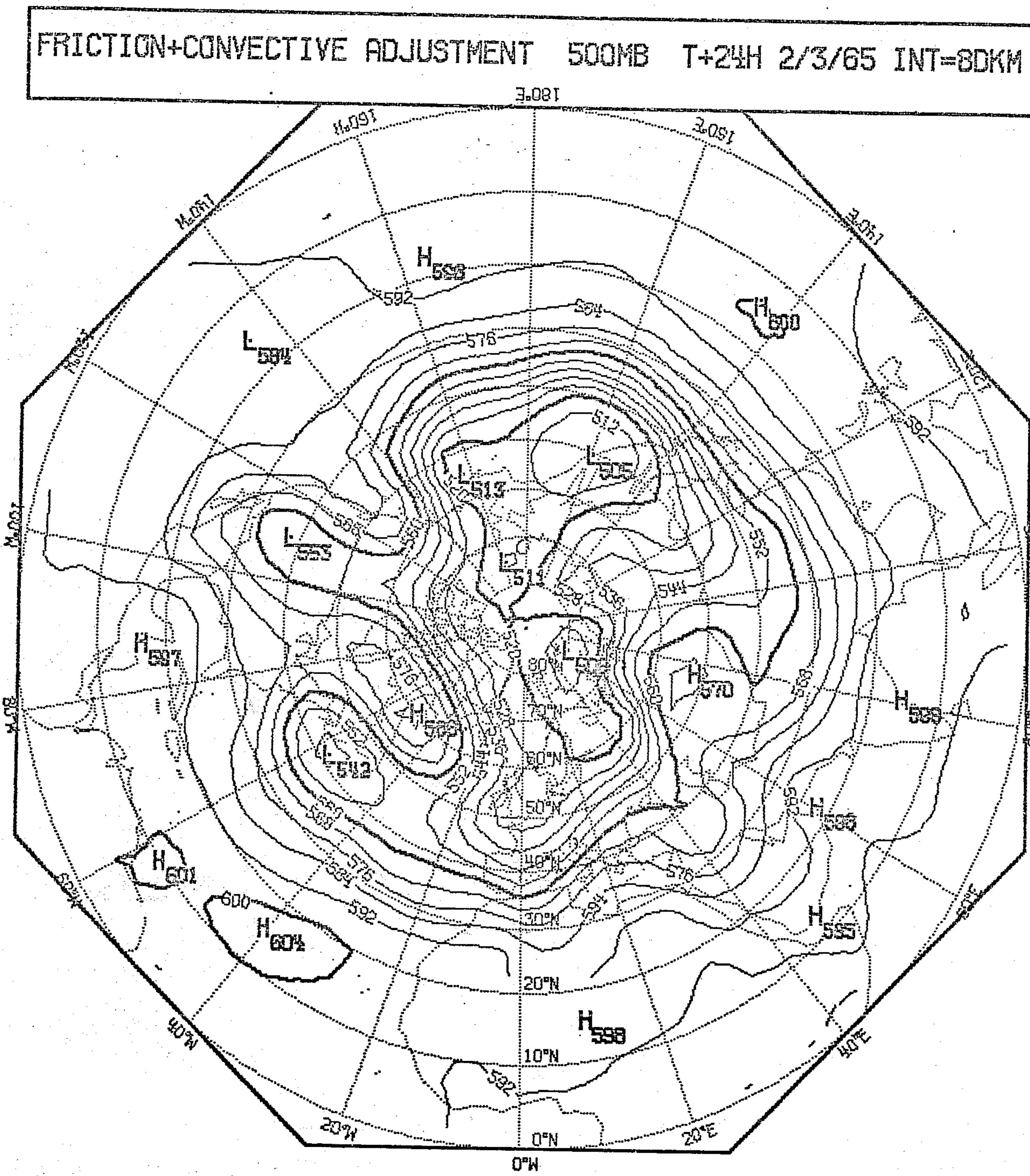
FRICTION+CONVECTIVE ADJUSTMENT 500MB T+24H 2/3/65 INT=8DKM
180°E
160°W
160°E
140°W
140°E
120°W
120°E
100°W
100°E
80°W
80°E
60°W
60°E
40°W
40°E
20°W
20°E
0°W
0°N
10°N
20°N
30°N
40°N
50°N
60°N
70°N
80°N

FIGURE 19

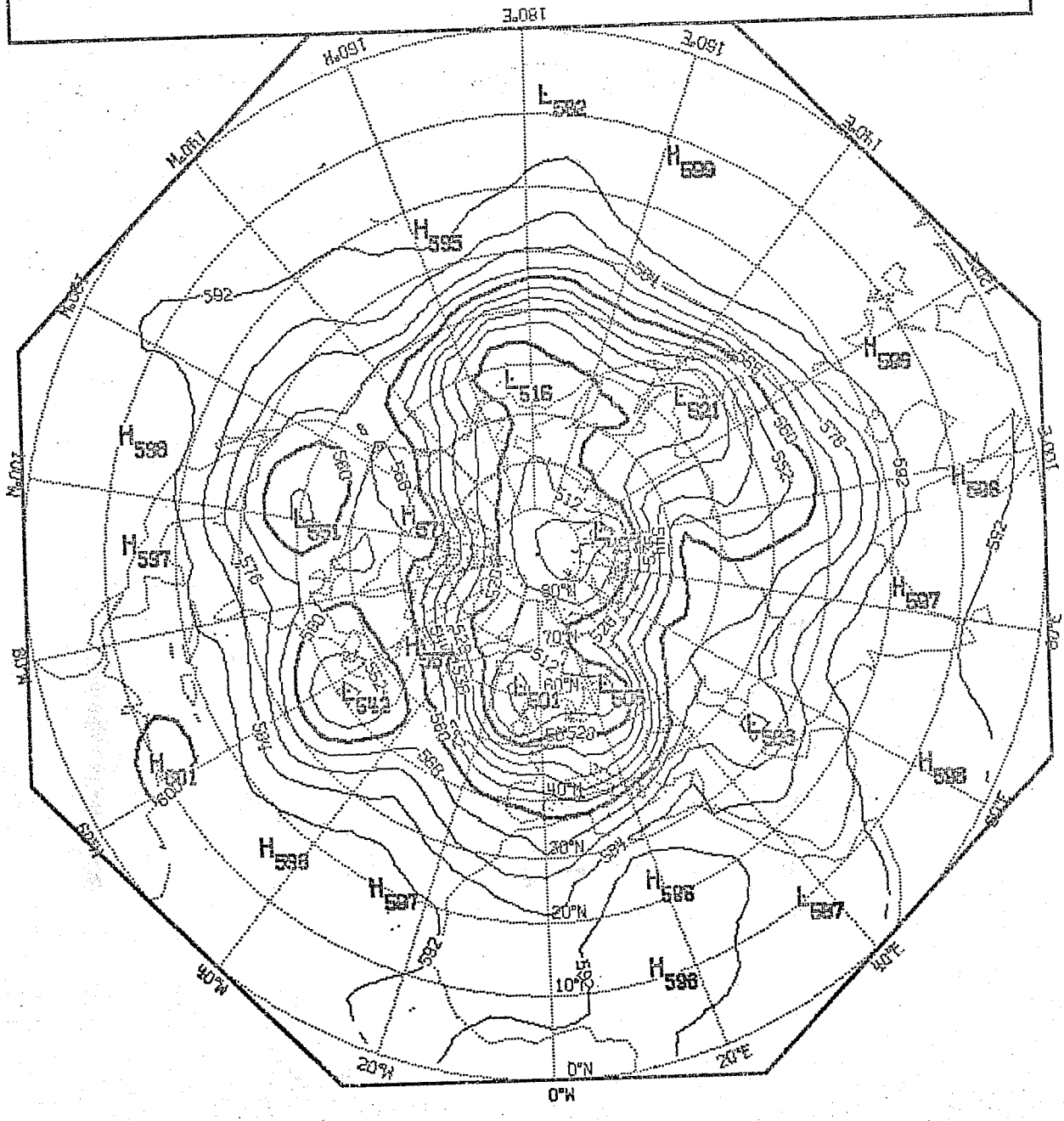
FRICTION+CONVECTIVE ADJUSTMENT 500MB T+72H 4/3/65 INT=8DKM
180°E
160°W
140°W
120°W
100°W
80°W
60°W
40°W
20°W
0°W
20°E
40°E
60°E
80°E
100°E
120°E
140°E
160°E
180°E
90°N
80°N
70°N
60°N
50°N
40°N
30°N
20°N
10°N
0°N
L 582
H 599
H 595
592
L 516
L 521
H 599
H 598
H 597
L 551
H 597
L 543
L 501
L 525
L 523
H 597
H 601
H 598
H 597
H 596
L 597
H 596
588
584
580
576
572
568
564
560
556
552
548
544
540
536
532
528
524
520
516
512

FIGURE 20

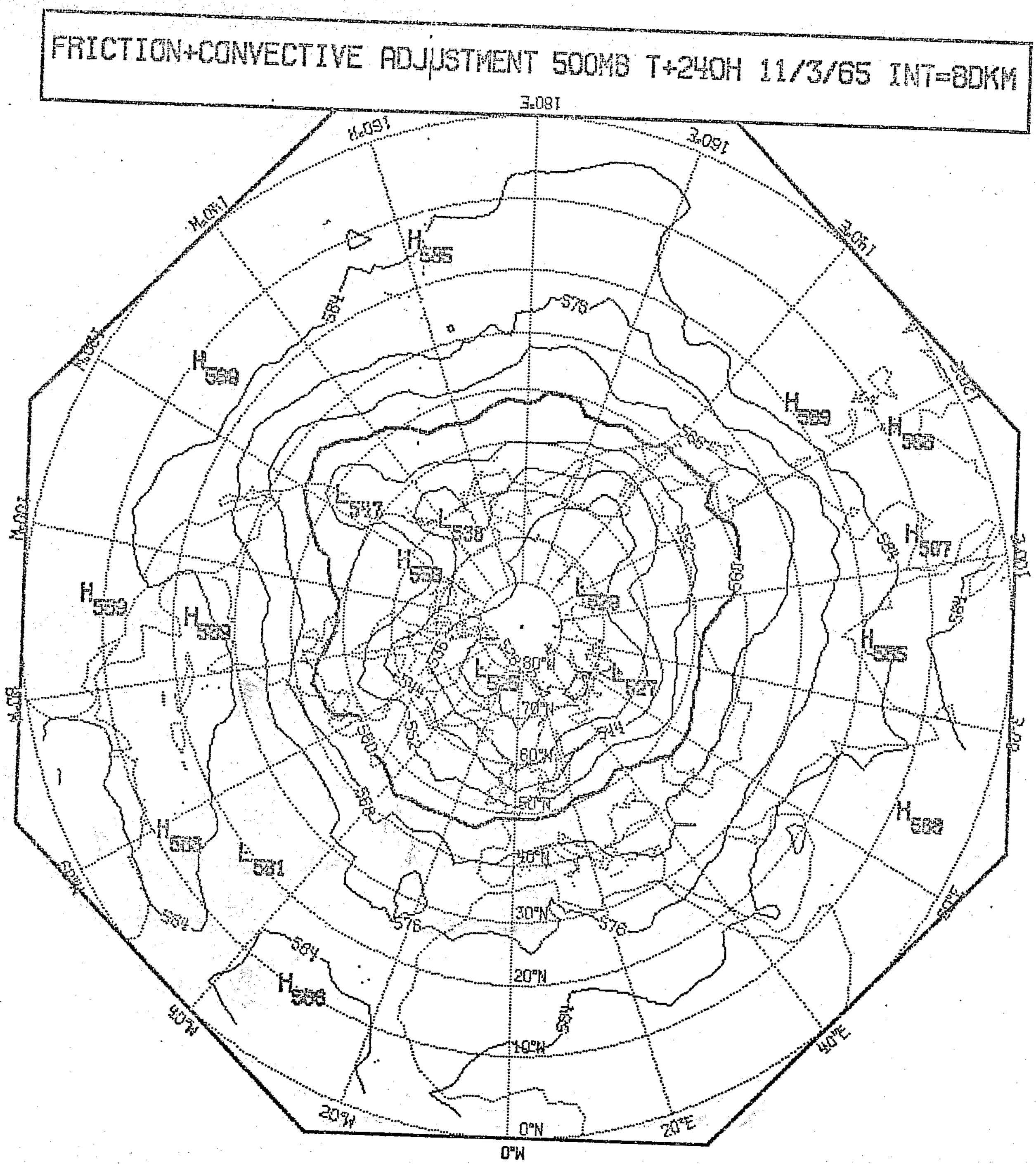
FRICTION+CONVECTIVE ADJUSTMENT 500MB T+240H 11/3/65 INT=8DKM

FIGURE 21

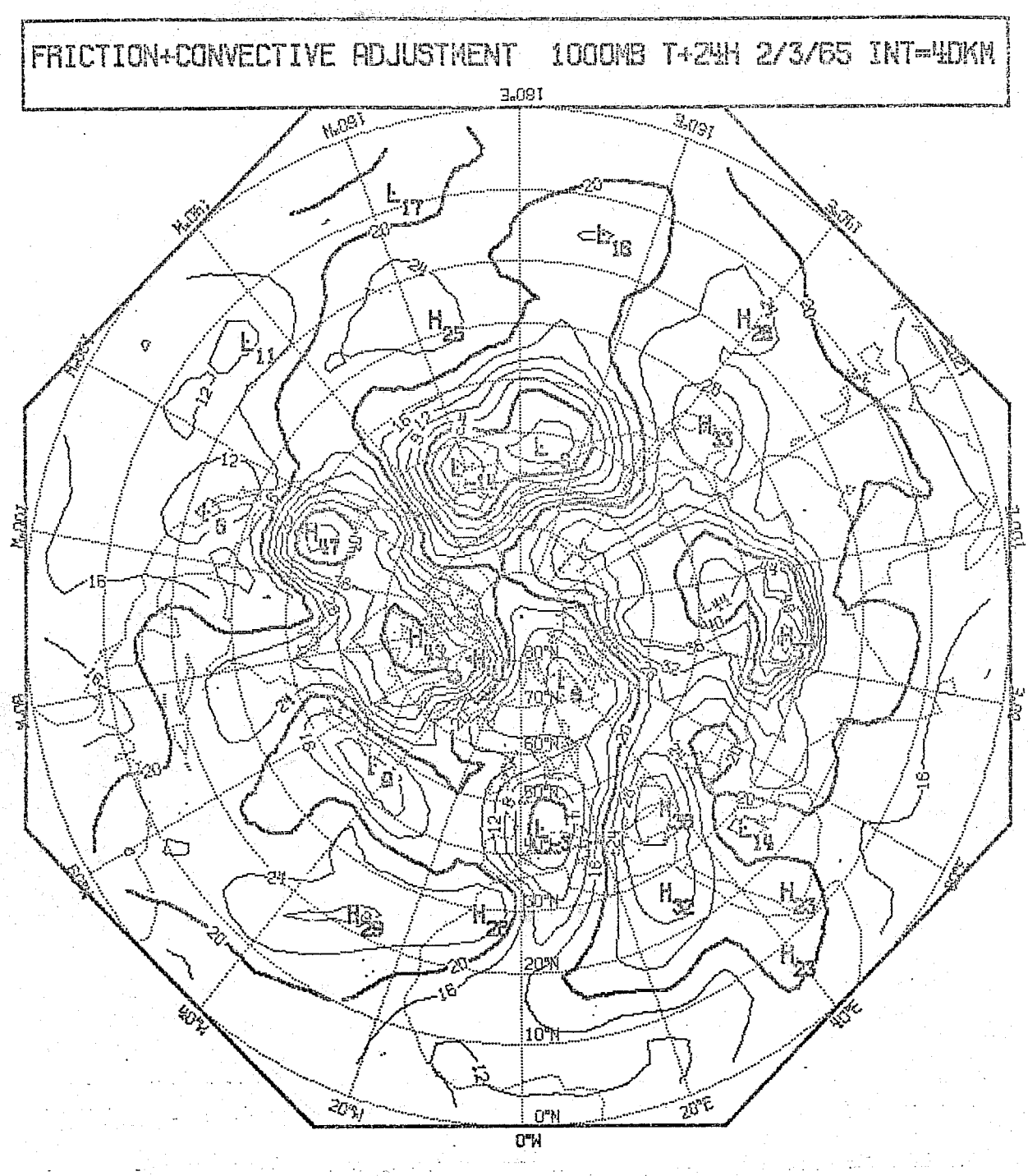
FRICTION+CONVECTIVE ADJUSTMENT 1000MB T+24H 2/3/65 INT=40KM
180°E
0°W
0°N
20°E
20°N
40°N
60°N
70°N
80°N
10°N

FIGURE 22

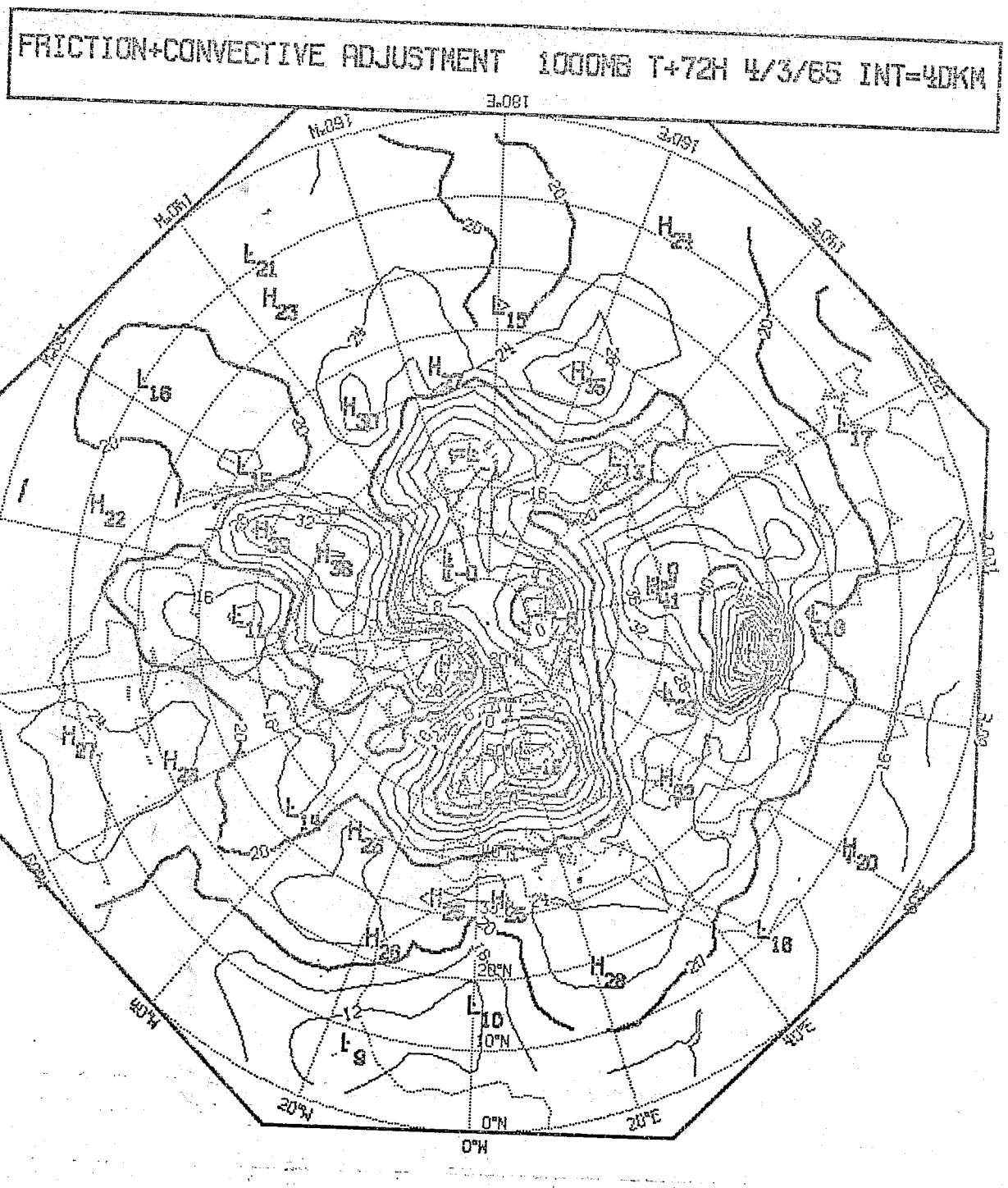
FRICTION+CONVECTIVE ADJUSTMENT 1000MB T+72H 4/3/65 INT=40KM
180°W
160°W
140°W
120°W
100°W
80°W
60°W
40°W
20°W
0°W
20°E
40°E
60°E
80°E
100°E
120°E
140°E
160°E
180°E
80°N
60°N
40°N
20°N
0°N
10°N
20°N
H21
L21
H23
L15
H24
H25
H26
L16
H30
L17
L13
H22
H27
H31
L18
L11
L19
H29
L14
H28
L20
H32
H33
L12
L10
L9

FIGURE 23

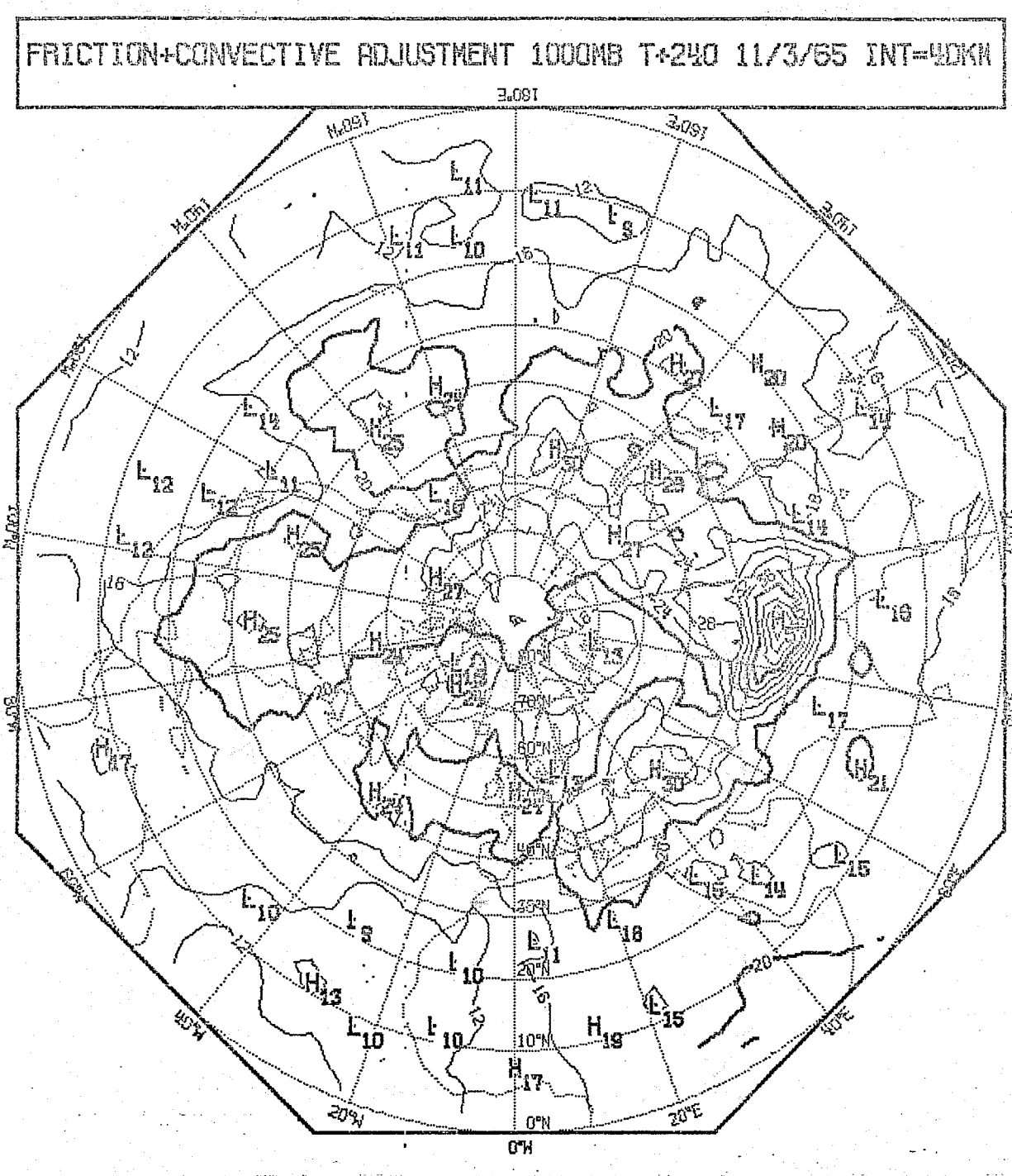

FIGURE 24

EUROPEAN CENTRE FOR
MEDIUM RANGE WEATHER
FORECASTS

Research Department (RD)

Technical Report No. 4

No. 1 A Case Study of a Ten Day Prediction

No. 2 The Effect of Arithmetic Precision on some Meteorological Integrations

No. 3 Mixed-Radix Fast Fourier Transforms without Reordering

No. 4 A Model for Medium Range Weather Forecasting - Adiabatic Formulation -